AD-A072 999 DAVID W TAYLOR NAVAL SHIP RESEARCH AND DEVELOPMENT CE--ETC F/G 20/4
PREDICTION OF DRAG COEFFICIENTS OF A SUPERSONIC V/STOL CONFIGUR--ETC(U)
AUG 79 T C TAI, T H BOYD, R E KUHN

UNCLASSIFIED DTNSRDC-79/074 NL

| OF |
AD
A072999

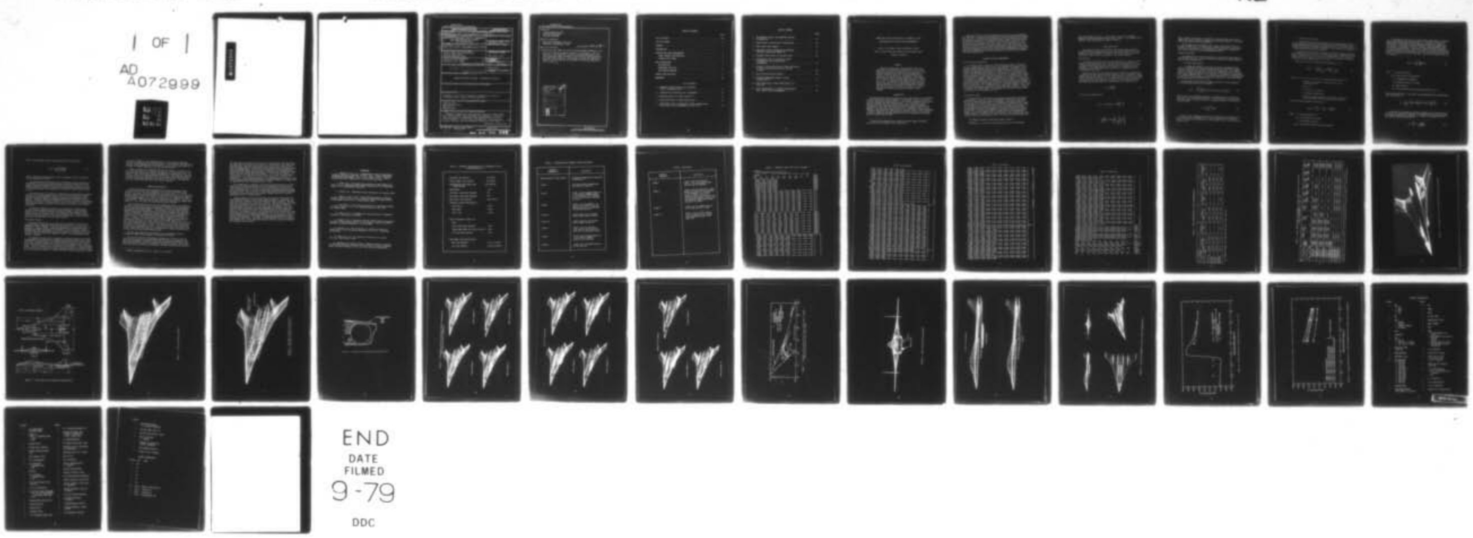

END
DATE
FILMED
9-79
DDC

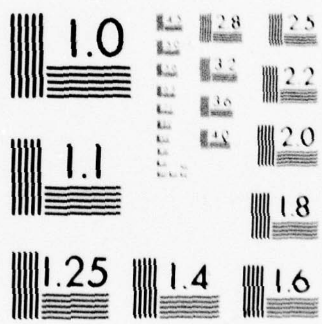

MICROCOPY RESOLUTION TEST CHART
NATIONAL BUREAU OF STANDARDS-1963-A

AD A072999

UNCLASSIFIED

SECURITY CLASSIFICATION OF THIS PAGE (When Data Entered)

REPORT DOCUMENTATION PAGE

READ INSTRUCTIONS BEFORE COMPLETING FORM

1. REPORT NUMBER: 14 DTNSRDC-79/074, DTNSRDC/AERO-1260

2. GOVT ACCESSION NO.

3. RECIPIENT'S CATALOG NUMBER

4. TITLE (and Subtitle): 6 PREDICTION OF DRAG COEFFICIENTS OF A SUPERSONIC V/STOL CONFIGURATION WITH VARIOUS STORE ARRANGEMENTS,

5. TYPE OF REPORT & PERIOD COVERED

6. PERFORMING ORG. REPORT NUMBER: Aero Report 1260 ✓

7. AUTHOR(s): 10 Tsze C./Tai, Thomas H./Boyd, ~~and~~ Richard E./Kuhn

8. CONTRACT OR GRANT NUMBER(s)

9. PERFORMING ORGANIZATION NAME AND ADDRESS:
David W. Taylor Naval Ship Research
and Development Center
Bethesda, Maryland 20084

10. PROGRAM ELEMENT, PROJECT, TASK AREA & WORK UNIT NUMBERS: (See reverse side)

11. CONTROLLING OFFICE NAME AND ADDRESS:
Naval Air Systems Command
Washington, D.C. 20361
(Continued on reverse side)

12. REPORT DATE: 11 Augu[redacted]979

13. NUMBER OF PAGES: 41 12 44p.

14. MONITORING AGENCY NAME & ADDRESS (if different from Controlling Office): 16 WR02302 17 WR0230201

15. SECURITY CLASS. (of this report): UNCLASSIFIED

15a. DECLASSIFICATION/DOWNGRADING SCHEDULE

16. DISTRIBUTION STATEMENT (of this Report)

APPROVED FOR PUBLIC RELEASE: DISTRIBUTION UNLIMITED

17. DISTRIBUTION STATEMENT (of the abstract entered in Block 20, if different from Report)

18. SUPPLEMENTARY NOTES

Presented at the 11th Navy Symposium on Aeroballistics, Naval Air Development Center, Trevose, PA (22-24 Aug 1978).

19. KEY WORDS (Continue on reverse side if necessary and identify by block number)

V/STOL Aircraft
Supersonic Wave Drag
Skin Friction
External Stores

20. ABSTRACT (Continue on reverse side if necessary and identify by block number)

Numerical computations, using supersonic area rule, linear theory and turbulent boundary layer solutions, were performed to evaluate the drag coefficients of a supersonic V/STOL configuration with various store arrangements. External stores included short- and medium-range missiles, electronic pod, and 600-gallon (2280-liters) fuel tanks.

(Continued on reverse side)

DD FORM 1 JAN 73 1473 EDITION OF 1 NOV 65 IS OBSOLETE
S/N 0102-LF-014-6601

UNCLASSIFIED

SECURITY CLASSIFICATION OF THIS PAGE (When Data Entered)

387 695

79 09 22 038

UNCLASSIFIED

SECURITY CLASSIFICATION OF THIS PAGE (When Data Entered)

(Block 10)

Program Element 6115-3N
Task Area WR 0230201
Work Unit 1606-300

WR 023 0 2

WR023 0201

(Block 11 continued)

Naval Air Development Center (60)
Warminster, Pennsylvania 18974

(Block 20 continued)

2 and 66.2 million per foot.

Predictions were based on cruise conditions at Mach numbers 1.2, 1.6, and 1.8 with Reynolds numbers between 2×10^6 and 66.2×10^6. As expected, it was found that the drag coefficient decreases as the free-stream Mach number increases. The wave drag varies nonlinearly with added store capacity. Data indicate that for the same store capacity, the wave drag may be minimized by judicious selection of store location.

Accession For	
NTIS GRA&I	✓
DDC TAB	
Unannounced	
Justification	
By	
Distribution/	
Availability Codes	
Dist	Avail and/or special
A	

UNCLASSIFIED

SECURITY CLASSIFICATION OF THIS PAGE (When Data Entered)

TABLE OF CONTENTS

LIST OF TABLES

LIST OF FIGURES

PREDICTION OF DRAG COEFFICIENTS OF A SUPERSONIC V/STOL

CONFIGURATION WITH VARIOUS STORE ARRANGEMENTS*

Tsze C. Tai, Thomas H. Boyd, and Richard E. Kuhn

David W. Taylor Naval Ship Research and Development Center

Bethesda, Maryland

ABSTRACT

Numerical computations, using supersonic area rule, linear theory and turbulent boundary layer solutions, were performed to evaluate the drag coefficients of a supersonic V/STOL configuration with various store arrangements. External stores included short- and medium-range missiles, electronic pod, and 600-gallon (2280-liters) fuel tanks. Predictions were based on cruise conditions at Mach numbers 1.2, 1.6, and 1.8 with Reynolds numbers between 2×10^6 and 66.2×10^6. As expected, it was found that the drag coefficient decreases as the free-stream Mach number increases. The wave drag varies nonlinearly with added store capacity. Data indicate that for the same store capacity, the wave drag may be minimized by judicious selection of store location.

INTRODUCTION

The drag prediction analysis reported in this paper was part of an evaluation to define the geometry and performance of a supercruiser concept for vertical and short takeoff and landing (V/STOL) to carry weapons compatible with the deck launched intercept (DLI) and strike missions. It is a modified version of a National Aeronautics and Space Administration (NASA) supercruise fighter configuration. An inboard profile was developed to integrate engines, fixed equipment, avionics, fuel, and landing gear in a preliminary design process. Changes in the fuselage were made to meet volume requirements, and new approaches to weapons integration were developed without adverse effects on the area distribution. Weapon and airframe integration must be accomplished with minimal effect on overall aircraft drag.

---

*This work was sponsored by the Naval Air Systems Command (AIR-320D) and the Naval Air Development Center (NADC-6051).

Drag coefficients of the new configuration with seven store arrangements were determined. Theoretical drag consists of supersonic wave drag and turbulent skin friction. The former was calculated either by a far-field solution based on supersonic area rule or by a near-field solution based on the linear theory. The latter was evaluated by a turbulent flat plate solution applied to local longitudinal strips aligned with a free stream. The shearing stress of these strips was determined with the Reynolds number based on the strip length; the frictional drag of the whole aircraft was obtained by summing those strip values. Computations were made at the David W. Taylor Naval Ship Research and Development Center (DTNSRDC) using an existing supersonic aircraft analysis program[1*] with minor modifications.

AIRCRAFT AND STORE ARRANGEMENTS

Clean Aircraft Configuration

The aircraft model is basically a NASA Supercruise Fighter 4[**] modified with twin extended pods at the rear end of the fuselage to accommodate fixed equipment without adverse effects on area distribution. The model is a twin-engine tailless arrow-wing design with a single rectangular inlet beneath the fuselage and outboard vertical tails and ventral fins. The original configuration, the NASA Supercruise Fighter 4, is a supersonic cruise concept aerodynamically designed for efficient cruise at Mach 1.8. An isometric and a three-view drawing of the present aircraft configuration are shown in Figures 1 and 2, respectively. Geometric characteristics are given in Table 1. A feature of this modified configuration is the extension of the fuselage at the fuselage-wing juncture and a short extension at the fuselage centerline between the engines. Modifications made to the fuselage contours, to accommodate engines sized for the mission applications, are not apparent in the three views. Figures 3 and 4 show the original and modified version of the NASA Supercruise Fighter 4. Figure 5 illustrates the revisions made to the fuselage cross section in Station 38.89 located just aft of the engine inlet face.

Aircraft with Stores

External stores of the aircraft configuration include short- and medium-range missiles, an electronic pod, and 600-gallon (2280-liters) fuel tanks. To avoid the high drag that would be encountered at supersonic speeds with conventional pylon mounted stores, an aerodynamically integrated store concept was envisaged. The stores were assumed to be reconfigured so that they could be flush mounted on the bottom of the aircraft and fitted with disposable fairings where necessary to aerodynamically integrate them with the lines of the airframe. They would thus appear as longitudinally oriented streamlined bulges. The computer program could not accept the actual aerodynamically designed stores configuration and it was necessary to use the equivalent body area distribution in predicting the drag. All stores are mounted symmetrically

---

[*]A complete listing of references is given on page 10.

[**]Reference 2 is cited for a detailed description of the NASA model.

about the fuselage centerline. A description of the store arrangement combinations and their designations are given in Table 2. The computer drawn figures of these combinations are shown in Figure 6.

DRAG CALCULATIONS

The theoretical drag of an aircraft in supersonic flight consists of the skin friction and the supersonic wave drag. Pressure drag due to flow separation is not considered. In addition, the present study is restricted to zero lift cases so that the drag due to lift is not presented.

Skin Friction

The total aircraft skin friction drag coefficient is a function of Mach number and Reynolds number values. The skin friction drag coefficient C_f of smooth and plane surfaces, as a function of Reynolds number Re_∞ is given in Figure 7. The figure, modified from Reference 3, represents average coefficients of 16 independent tests. The effect of compressible flow is to reduce the value of C_f.

The skin friction of the configurations with stores was computed using a turbulent flat plate solution which is applied to local longitudinal strips aligned with the free stream. The flat plate solution is called the T method which is based on the calculation of a compressible skin friction coefficient C_f from a reference skin friction coefficient C'_f for a given free-stream Mach number M_∞, Reynolds number Re_∞, and adiabatic wall temperature T_w:

$$C_f = C'_f\left(\frac{T_\infty}{T'}\right) \tag{1}$$

T' and C'_f are obtained from

$$\frac{T'}{T_\infty} = 1 + 0.035M_\infty^2 + 0.45\left(\frac{T_w}{T_\infty} - 1\right) \tag{2}$$

$$\frac{0.242}{(C'_f)^{1/2}} = \log_{10}\left[C'_f\,\frac{Re_\infty}{\left(\frac{T'}{T_\infty}\right)^{1+\omega}}\right] \tag{3}$$

where ω denotes the exponent of Sutherland's relation between viscosity and temperature, and the subscript ∞ denotes the free-stream condition. The derivation of the method is given in Reference 4.

The configuration, including the tail, canard, and external stores, is divided into many strips; the wetted area of these strips are then calculated. The total frictional drag of the configuration is determined by summing the strip values along with the corresponding wetted areas.

Supersonic Wave Drag

The supersonic wave drag was calculated by a far-field solution based on the supersonic area rule. A near-field solution based on the linear theory was used as a check in some cases.

1. The Far-Field Solution

In using the supersonic area rule, the aircraft configuration with stores is transformed into several equivalent bodies of revolution by passing a series of parallel cutting planes through the configuration. The cutting planes are inclined with respect to the aircraft longitudinal axis at the Mach angle, and a single equivalent body is produced for the series of cutting planes at a constant azimuthal angle θ. The cross-sectional area of the equivalent body at each station is the projection of the area intercepted by the cutting plane onto a plane normal to the aircraft axis.

The wave drag of each equivalent body of revolution is then determined by the slender-body relation of von Kármán[5]:

$$D(\theta) = -\frac{\rho V_\infty^2}{4\pi}\int_0^\ell\int_0^\ell A''(x_1)\, A''(x_2)\, \log\, |x_1-x_2|\, dx_1 dx_2 \tag{4}$$

where x_1 and x_2 are lengthwise variables of integration and A'' is the second derivative of the body area distribution. The wave drag of the aircraft at a given Mach number is calculated from the integrated average of the equivalent-body wave drags.

$$D = \frac{1}{2\pi}\int_0^{2\pi} D(\theta)\, d\theta \tag{5}$$

Because of the configuration generality possessed by the supersonic area rule, various store arrangements can be easily transformed into equivalent bodies of revolution and, therefore, it is the primary source for obtaining the zero-lift wave.

2. The Near-Field Solution

The accuracy of the far-field solution was first checked by a more sophisticated near-field solution which gives more detailed information such as surface pressure distribution and interference effects. The entire solution involves calculations of "isolated" wave drag of the components and superposition of interference drag between the components.

In calculating the "isolated" wave drag, the surface pressure coefficient on the upper (or lower) surface of a flat-mean-line wing of symmetrical surface shape is obtained by first determining the corresponding velocity potential, differentiating with respect to x (to get u), and then computing the pressure coefficient from the approximation, $C_p = -2u/V_\infty$.

The velocity potential computation, from Reference 6, is:

$$\phi(x_1 y) = -\frac{1}{\pi}\iint_\tau \frac{\lambda d\eta d\xi}{\left[(x-\xi)^2 - \beta^2(y-\eta)^2\right]^{1/2}} \tag{6}$$

where ϕ (x,y) = velocity potential at a defined wing field point (x,y)

λ = surface slope (dz/dx) of wing section at a wing integration point

$\beta = (M_\infty^2-1)^{1/2}$

ξ = x variable of integration

η = y variable of integration

τ = subscript denoting interval of integration (surface of the wing planform within the Mach forecone from x,y)

The wing thickness pressure coefficient is:

$$C_p(x,y) = \frac{p-p_\infty}{q_\infty} = -\frac{2u}{V_\infty} = -2\frac{\partial\phi(x,y)}{\partial x} \tag{7}$$

where p = local pressure at x,y

p_∞ = free-stream static pressure

u = x perturbation velocity

U_∞, q_∞ = free-stream velocity and dynamic pressure

For fuselage and nacelles, the surface pressure distribution is obtained from a method based on the Lighthill theory.[7] The method is applicable to bodies having either smooth area distributions or bodies with slope discontinuities. In computation, smooth area distributions are assumed except (if required) at the nose or aft end of the body. Open-nose bodies, such as nacelles, are permissible. The solution technique requires calculating an axial perturbation velocity which is a function of the body cross-sectional area growth (and radius distribution) and a decay function which relates area growth to its effect on a given field point. The axial perturbation velocity u is given by:

$$u(x) = -\frac{1}{2\pi}\int_{0}^{x} \frac{W(z)}{\beta R_{\xi}}\, dS'_{\xi} \tag{8}$$

where x = body field station

W(Z) = decay function; see Reference 1

ξ = x variable of integration

Z = position function = $(x-\xi)/\beta R_{\xi}$

R_{ξ} = body radius at ξ

S'_{ξ} = first derivative of body cross-sectional area S at ξ

The pressure coefficient is calculated from one-dimensional flow relationships given in Reference 8.

$$C_p = \frac{1}{0.7M_{\infty}^2}\left(\left\{1+0.2M_{\infty}^2\left[(1+R'^2)(1+u)^2-1\right]\right\}^{3.5}-1\right) \tag{9}$$

To account for the pressure signatures propagated by the shock wave flow field about the fuselage and nacelles, the pressure field is calculated using the modified linear theory of Whitham for a supersonic axisymmetric flow.[8] The resultant pressure coefficient is

$$C_p = \frac{p-p_{\infty}}{q_{\infty}} = \frac{2F(y)}{(2\beta r)^{1/2}} \tag{10}$$

where r is the radial distance from the body and the function F(y)

$$F(y) = \frac{1}{2\pi}\int_0^y \frac{S''(t)dt}{(y-t)^{1/2}} \tag{11}$$

which is dependent on body geometry as S''(t) represents the second derivative of body cross-sectional area.

In calculating the interference drag, the fuselage-on-wing interference is determined by the near-field pressure signature from the fuselage at selected spanwise stations and imposing them upon the corresponding wing sections. The wing-on-fuselage interference is obtained by computing wing thickness pressures in the area occupied by the fuselage, with wing surface slopes being set equal to zero.

The nacelle-on-wing interference is obtained by calculating nacelle pressure signatures at the same spanwise stations used for the wing thickness pressures (plus extra stations immediately adjacent to the nacelle centerlines), then defining a composite signature by summing together the contributions from all nacelles. The nacelle pressure coefficients are doubled to account for reflection from the wing surface. The wing-on-nacelle term is accounted for by transferring wing thickness pressures along Mach lines from the wing surface to the nacelle centerline.

The nacelle-on-fuselage interference is considered by integrating each nacelle's pressure signature upon the fuselage area growth. The fuselage-on-nacelle term is obtained by imposing the fuselage pressure signature on each nacelle surface as a buoyancy force. The interference term of other nacelles acting on a selected nacelle is calculated by building up the composite buoyancy field, and then imposing it upon the nacelle surface.

The Computer Program

The computer program used for the above drag calculations is basically the supersonic aircraft analysis program described by Middleton et al. with minor modifications made at DTNSRDC. A detailed description of the program is given in Reference 1. Program options include the SKIN FRICTION, FAR-FIELD WAVE DRAG, NEAR-FIELD WAVE DRAG, WING DESIGN, LIFT ANALYSIS, and PLOT programs. Except for the WING DESIGN and LIFT ANALYSIS options, the program is fully utilized in this analysis. The PLOT routines were modified to adapt to the CALCOMP 936 plotting facility at DTNSRDC.

In preparing the inputs for the computer, the aircraft configuration surface is approximated by a large number of quadrilateral shapes defined by input coordinate points in physical space. The original fuselage contour lines were modified to provide the volume requirements for mission oriented equipment, fuel, and engines. The mission oriented stores (missiles) were redesigned to obtain integrated stores. Then the resulting store configurations were converted to equivalent bodies of revolution and the radius determined at longitudinal stations as computer input data as illustrated in Figure 8. A sample listing of computer inputs for the V/STOL

5 is given in Table 3. The corresponding plots of four oblique orthographic views of the configuration are shown in Figure 9. These pictures are significant not only to show extensive flow calculation but also to offer an efficient way of checking the computer modeling of the selected configuration.

About 15 minutes of CDC 6600/6700 CPU time is required to calculate a far-field wave drag solution of a typical configuration at one angle of attack. The near-field wave drag solution requires approximately the same computer time even though it gives a more detailed pressure distribution. The reason for using the far-field solution for most cases is the ease in simulating the external stores by bodies of revolution associated with the area rule concept. The computing time for turbulent skin friction is less than two minutes.

RESULTS AND DISCUSSION

The drag coefficients were determined for the present supersonic V/STOL configuration with seven store arrangements and for the original NASA Supercruiser 4 test case. Wave drag values were calculated at $M_\infty = 1.2$, 1.6, and 1.8, and skin friction values were determined at the same Mach number with corresponding Reynolds numbers of 6.62×10^7, 5.88×10^7, and 4.41×10^7, respectively, based on a mean chord length of 31.06 feet (9.47 meters) and an altitude h = 50,000 feet (15,240 meters). Additional skin friction values were evaluated for subsonic Mach numbers 0.1, 0.2, 0.3, and 0.6 at additional but lower altitudes.

The calculated results of the test case (NASA Supercruiser 4) are presented in Table 4 and plotted in Figure 10 along with independently calculated data by Shrout* using the separate methods of References 4, 9, and 10, and experimental measurements taken from Reference 2. Skin friction, wave drag (which includes pressure drag and interference drag by the near-field solution), and drag due to camber are considered. Because the present supersonic V/STOL configuration has the same wing as the original NASA configuration, the values for drag due to camber at zero lift were taken directly from NASA calculations* for camber correction. Generally, the present calculated results compare very well with the experimental values at $M_\infty = 1.6$ and 1.8, but yield higher values at $M_\infty = 1.2$. This is expected because the linear theory starts to fall apart as the free-stream Mach number approaches unity. However, the accuracy of the linear theory may be improved to a certain extent by using a fine integration grid, as done by Shrout to yield better comparison at $M_\infty = 1.2$. Figure 10 also shows some subsonic drag values. Because the theory does not include drag due to camber, the results are considerably lower than actual measured values.

The basic data computed in the present work are summarized in Table 5. Configuration numbers are designated in accordance with Table 2.

For the clean aircraft configuration, Configuration 1, both far-field and near-field wave drag values were determined and the difference between the two solutions was examined. Basically, the far-field solution yields slightly higher wave drag values than the near-field solution (including the camber correction). Since the near-field solution is considered to be more reliable and more accurate,

---

*Private communication with B.L. Shrout on 26 Jan 1978.

the total drag is determined by the sum of the near-field wave drag (including the camber correction) and the skin friction. Configuration 1 has larger total wetted area and, therefore, yields higher wave drag as well as skin friction. Note that computations of skin friction for the original NASA configuration were based on Reynolds number 2×10^6 while calculations for other configurations were based on much higher Reynolds number, determined by the combination of Mach number, altitude, and the mean chord length, $c = 31.06$ feet (9.47 meters). At an altitude of $h = 50{,}000$ feet (15,240 meters), the resultant Reynolds number would be 6.62×10^7, 5.88×10^7 and 4.41×10^7 for $M_\infty = 1.8$, 1.6, and 1.2, respectively. At these Reynolds numbers, the corresponding skin friction results for the original NASA configuration would be 0.00467, 0.00496, and 0.00559, which are generally lower than the Configuration 1 values.

For Configurations 2 through 9, the wave drag coefficients were all determined by the far-field solution which were then converted to the near-field values based on correlation between the coefficients obtained by the two solutions for Configuration 1. The total drag coefficients were obtained by adding the skin friction. The total drag, so determined, should therefore include the interference drag and the drag due to camber, although they are not directly determined from the far-field solution.

Finally, Figure 11 depicts the variation of total drag coefficients with free-stream Mach numbers, using the data taken from Table 5. As expected, the drag coefficient decreases as the free-stream Mach number increases. The wave drag varies nonlinearly with added store capacity. This variation may be attributed to the interference of shock waves and to the difference in resulting equivalent bodies of revolution in accordance with the supersonic area rule. This difference implies that an optimum arrangement of external stores can be found to yield an equivalent body of revolution having the least supersonic wave drag. For instance, at $M_\infty = 1.8$, the drag value of the aircraft with four medium range air-to-air missiles (Configuration 3) is 0.01102 and the drag value of the aircraft with four identical missiles plus two short range air-to-air missiles (Configuration 5) is 0.01099. The wave drag decreases when two short range missiles were added. The results of Configurations 3 and 3A (in Table 5) also indicate that, for the same store capacity, the wave drag may be minimized with judicious store location.

REFERENCES

1. Middleton, W.D. et al., "A Computational System for Aerodynamic Design and Analysis of Supersonic Aircraft: Part 1 - General Description and Theoretical Development; Part 2 - User's Manual; Part 3 - Computer Program Description," NASA CR-2715, 2716, and 2727 (Jul 1976).

2. Shrout, B.L., "Aerodynamic Characteristics at Mach Numbers from 0.6 to 2.16 of a Supersonic Cruise Fighter Configuration with a Design Mach Number of 1.8," NASA TM-X3559 (Sep 1977).

3. Hoerner, S.F., "Aerodynamic Drag," published by S.F. Hoerner (1951).

4. Sommer, C. and J. Short, "Free Flight Measurements of Turbulent Boundary Layer Skin Friction in the Presence of Severe Aerodynamic Heating at Mach Numbers from 2.8 to 7.0," NACA TN-3391 (1955).

5. Von Karman, T., "The Problem of Resistance in Compressible Fluids," R. Accad. d'Italia, Cl. Sci. Fis., Matematiche Naturali, Vol. XIII, pp. 210-265 (1935).

6. Lomax, H. et al., "Integrals and Integral Equations in Linearized Wing Theory," NACA Report 1054 (1950).

7. Lighthill, M.J., "Supersonic Flow Past Slender Bodies of Revolution, the Slope of Whose Meridian Section is Discontinuous," Quarterly Journal of Mechanics and Applied Mathematics I, Vol. 90 (1948).

8. Whitham, G.B., "The Flow Pattern of a Supersonic Projectile," Communications on Pure and Applied Mathematics, Vol. V, No. 2 (Aug 1952), pp. 301-348.

9. Harris, R.V., Jr., "An Analysis and Correlation of Aircraft Wave Drag," NASA TM-X-947 (1964).

10. Middleton, W.D. and H.W. Carlson, "Numerical Method of Estimating and Optimizing Supersonic Aerodynamic Characteristics of Arbitrary Planform Wings," Journal of Aircraft, Vol. 2, No. 4, pp. 261-265 (Jul-Aug 1965).

TABLE 1 - GEOMETRIC CHARACTERISTICS OF SUPERSONIC V/STOL CONFIGURATION NO. 1

Wing Span, feet (meters)	50 (15.24)
Overall Length, feet (meters)	65 (19.81)
Wing Reference Area, square feet (square meters)	1060 (98.513)
Aspect Ratio	2.08
Wing Sweep, Inner Panel (degrees)	72.5
Wing Sweep, Outer Panel (degrees)	45.6
Mean Chord c, feet (meters)	31.06 (9.467)
Outboard to Inboard Chord Ratios, τ	
Inner Panel	0.3272
Outer Panel	0.6145
Root to Tip	0.2010
Airfoil Thickness to Chord, t/c Ratio	
Root (0.2037 span) (percent)	2.488
Leading Edge Break (0.60 span) (percent)	3.360
Tip (1.00 span) (percent)	3.360
Wing Camber (see tabulated data)	
Root, feet (meters)	-2.417 (-0.7367)
Tip, feet (meters)	-0.1465 (-0.04465)

TABLE 2 - DESIGNATION OF EXTERNAL STORE ARRANGEMENT

Aircraft Designation	Description
NASA Supersonic Cruise Fighter 4	The model configuration as described in Reference 2.
V/STOL 1	The clean aircraft configuration as presented in Figure 2.
V/STOL 2	V/STOL 1 with two medium-range air-to-air missiles (MRAAM) mounted on the underside of the fuselage at the aircraft center of gravity location.
V/STOL 3	V/STOL 1 with four MRAAM's, two mounted as in V/STOL 2, and two mounted outboard at approximately the mid-wing location.
V/STOL 3A	V/STOL 3 with the two fuselage mounted MRAAM's moved forward.
V/STOL 3B	V/STOL 3 with the two fuselage mounted MRAAM's moved aft.
V/STOL T	V/STOL 1 with two 600-gallon (2280 liters) tanks mounted outboard near the mid-wing location.
V/STOL 5	V/STOL 3 with two short-range air-to-air missiles (SRAAM's) mounted on the wing tips.
V/STOL 6	V/STOL 2 with two SRAAM's mounted on the wing tips.

TABLE 2 (Continued)

Aircraft Designation	Description
V/STOL 7	V/STOL 3 with two 600-gallon (2280 liters) tanks mounted under the wing near the fuselage.
V/STOL 8	V/STOL 1 with one electronic counter measure pod mounted on the underside of the fuselage at the aircraft center of gravity, two air-to-surface missiles (ASM's) mounted outboard near the mid-wing location, and two 600-gallon (2280 liters) tanks mounted as in V/STOL 7.
V/STOL 9	V/STOL 8 with two SRRAM's mounted on the wing tips and no tanks.
V/STOL 10	V/STOL 1 with two ASM's mounted under the wing near the fuselage and two SRAAM's mounted on the wing tips.

TABLE 3 - NUMERICAL MODEL FOR V/STOL AIRCRAFT 5

```
GEOM NEW
  TYPE 8 SUPERSONIC V/STOL AIRCRAFT NO. 5
  1  1  1  1  1          8 18  4 16 10 20  8 23  8 25 10  3 19  2 10
1996.00                                                                 REFA
0.0     .5      1.5     5.0     10.     20.     30.     40.     50.     60.       XAF10
65.     70.     75.     80.     85.     90.     95.     100.                      XAF18
 27.178  6.985 -1.715 52.118                                            WORG1
 32.421  9.572 -1.999 47.112                                            WORG2
 43.244 12.001 -2.667 36.860                                            WORG3
 52.995 15.430 -3.104 27.681                                            WORG4
 57.473 17.165 -3.277 23.490                                            WORG5
 65.626 20.554 -3.429 17.051                                            WORG6
 65.626 20.574 -3.429 17.051                                            WORG7
 79.057 34.290 -3.335 10.478                                            WORG8
  0.000   .023   .081   .211   .221  -.051  -.470  -.975 -1.377 -1.908  TZ 1
 -2.129 -2.324 -2.504 -2.687 -2.858 -3.020 -3.183 -3.315                TZ 1
  0.000   .028   .086   .234   .251   .030  -.348  -.787 -1.242 -1.681  TZ 2
 -1.892 -2.096 -2.286 -2.477 -2.647 -2.799 -2.972 -3.104                TZ 2
  0.000   .023   .069   .206   .279   .216   .020  -.239  -.528  -.836  TZ 3
  -.988 -1.138 -1.288 -1.435 -1.575 -1.712 -1.844 -1.968                TZ 3
  0.000   .018   .048   .165   .239   .262   .185   .063  -.089  -.264  TZ 4
  -.356  -.450  -.544  -.640  -.734  -.825  -.917 -1.003                TZ 4
  0.000   .013   .041   .124   .216   .264   .231   .163   .063  -.053  TZ 5
  -.117  -.180  -.246  -.310  -.376  -.439  -.505  -.566                TZ 5
  0.000   .005   .013   .041   .081   .109   .104   .081   .046   .005  TZ 6
  -.015  -.041  -.066  -.091  -.119  -.147  -.173  -.201                TZ 6
  0.000   .005   .013   .041   .081   .109   .104   .081   .046   .005  TZ 7
  -.015  -.041  -.066  -.091  -.119  -.147  -.173  -.201                TZ 7
  0.000  -.003  -.008  -.028  -.056  -.074  -.079  -.074  -.061  -.041  TZ 8
  -.023  -.008   .013   .030   .051   .071   .094   .117                TZ 8
0.0     .338    .529    .628    .750    .944    1.078   1.166   1.220   1.244     WORD 1
1.216   1.150   1.049   .912    .738    .528    .283    0.0                       WORD 1
0.0     .354    .536    .658    .786    .990    1.130   1.222   1.278   1.304     WORD 2
1.274   1.206   1.099   .959    .774    .554    .296    0.0                       WORD 2
0.0     .400    .602    .743    .888    1.118   1.276   1.379   1.442   1.472     WORD 3
1.438   1.362   1.241   1.079   .873    .626    .334    0.0                       WORD 3
0.0     .462    .694    .857    1.022   1.287   1.470   1.589   1.662   1.696     WORD 4
1.657   1.569   1.430   1.243   1.006   .721    .385    0.0                       WORD 4
0.0     .470    .706    .873    1.042   1.311   1.498   1.619   1.694   1.728     WORD 5
1.688   1.598   1.457   1.266   1.025   .734    .392    0.0                       WORD 5
0.0     .457    .687    .849    1.013   1.275   1.457   1.574   1.646   1.680     WORD 6
1.642   1.554   1.416   1.231   .996    .714    .382    0.0                       WORD 6
0.0     .034    .098    .319    .605    1.075   1.411   1.613   1.680   1.613     WORD 7
1.529   1.411   1.260   1.075   .857    .605    .319    0.0                       WORD 7
0.0     .034    .098    .319    .605    1.075   1.411   1.613   1.680   1.613     WORD 8
1.529   1.411   1.260   1.075   .857    .605    .319    0.0                       WORD 8
  0.000   .953  1.905  3.810  5.649  7.620  9.525 11.430 14.605 15.240  XFUS  10
  0.000  0.000  0.000  0.000  0.000  0.000  0.000  0.000  0.000  0.000  Y      1
  0.000  0.000  0.000  0.000  0.000  0.000                              Y      1
 -3.310 -3.310 -3.310 -3.310 -3.310 -3.310 -3.310 -3.310 -3.310 -3.310  Z      1
 -3.310 -3.310 -3.310 -3.310 -3.310 -3.310                              Z      1
  0.000   .094   .196   .272   .323   .399   .450   .475   .503   .503  Y      2
   .503   .376   .272   .145   .043  0.000                              Y      2
 -3.640 -3.614 -3.538 -3.487 -3.386 -3.284 -3.233 -3.208 -3.157 -3.106  Z      2
 -3.056 -3.056 -3.056 -3.056 -3.078 -3.078                              Z      2
  0.000   .178   .305   .434   .460   .536   .615   .640   .716   .792  Y      3
   .640   .513   .335   .183   .056   0.00                              Y      3
 -3.716 -3.665 -3.566 -3.439 -3.312 -3.185 -3.109 -3.033 -2.957 -2.968  Z      3
 -2.880 -2.855 -2.852 -2.878 -2.875 -2.875                              Z      3
  0.000   .178   .406   .559   .663   .790   .866   .942  1.146  1.222  Y      4
  1.120   .841   .584   .330   .127   0.0                                Y      4
 -3.995 -3.945 -3.818 -3.716 -3.538 -3.155 -2.977 -2.926 -2.774 -2.697  Z      4
```

TABLE 3 (Continued)

-2.621	-2.545	-2.520	-2.494	-2.494	-2.469					Z	4
0.000	.406	.739	.917	.993	1.120	1.171	1.247	1.425	1.476	Y	5
1.374	1.019	.688	.406	.229	0.00					Y	5
-4.199	-4.097	-3.868	-3.716	-3.538	-3.002	-2.901	-2.799	-2.596	-2.520	Z	5
-2.393	-2.342	-2.215	-2.139	-2.088	-2.062					Z	5
0.000	.518	.978	1.133	1.311	1.491	1.516	1.570	1.697	1.798	Y	6
1.671	1.316	.935	.655	.249	0.0					Y	6
-4.326	-4.176	-3.896	-3.747	-3.442	-2.753	-2.652	-2.576	-2.423	-2.322	Z	6
-2.195	-2.068	-1.913	-1.732	-1.605	-1.577					Z	6
0.00	.493	1.001	1.435	1.615	1.847	1.900	1.976	2.205	2.230	Y	7
2.106	1.671	1.214	.782	.427	0.0					Y	7
-4.376	-4.277	-4.051	-3.772	-3.442	-2.603	-2.451	-2.400	-2.197	-2.096	Z	7
-1.968	-1.814	-1.582	-1.351	-1.199	-1.171					Z	7
0.000	.841	1.450	1.755	1.935	2.164	2.266	2.367	2.621	2.697	Y	8
2.621	1.882	1.374	.866	.406	0.0					Y	8
-4.481	-4.300	-3.995	-3.767	-3.437	-2.520	-2.393	-2.266	-2.139	-1.986	Z	8
-1.831	-1.501	-1.222	-0.917	-.765	-.739					Z	8
0.000	1.095	2.012	2.240	2.367	2.799	2.901	3.028	3.437	3.564	Y	9
3.360	2.672	1.831	1.196	.610	0.0					Y	9
-4.455	-4.326	-3.995	-3.919	-3.767	-2.443	-2.164	-2.062	-1.961	-1.755	Z	9
-1.552	-1.196	-.765	-.330	-.076	0.0					Z	9
0.000	1.029	1.971	2.250	2.431	2.791	2.944	3.200	3.658	3.683	Y	10
3.609	3.025	2.060	1.323	.663	0.0					Y	10
-4.427	-4.305	-4.079	-3.876	-3.647	-2.504	-2.200	-2.047	-1.872	-1.768	Z	10
-1.539	-1.283	-.770	-.259	.048	.178					Z	10
15.240	16.192	17.145	19.050	21.438	25.717	27.178	29.528			XFUS	8
0.000	1.001	1.948	2.233	2.441	2.791	2.924	3.101	3.282	3.668	Y	1
3.721	3.647	3.266	2.154	1.146	.968	.765	.485	.231	0.0	Y	1
-4.437	-4.326	-4.061	-3.861	-3.609	-2.494	-2.215	-2.116	-2.042	-1.895	Z	1
-1.768	-1.590	-1.405	-.851	-.198	-.091	-.013	.094	.124	.152	Z	1
0.000	.958	2.007	2.289	2.522	2.896	3.028	3.157	3.310	3.823	Y	2
3.955	3.780	3.475	2.261	1.351	1.125	.925	.546	.213	0.0	Y	2
-4.437	-4.374	-4.110	-3.934	-3.734	-2.515	-2.314	-2.187	-2.088	-1.867	Z	2
-1.715	-1.483	-1.300	-.696	-.397	.213	.498	.681	.737	.739	Z	2
0.000	.932	1.979	2.492	2.751	3.099	3.231	3.490	3.693	4.155	Y	3
4.262	4.135	3.731	2.642	1.554	1.410	1.135	.782	.401	0.0	Y	3
-4.488	-4.399	-4.237	-4.013	-3.686	-2.596	-2.291	-2.090	-2.017	-1.819	Z	3
-1.593	-1.463	-1.227	-.701	-.099	.516	.902	1.161	1.321	1.377	Z	3
0.000	1.128	2.329	2.766	2.974	3.376	3.533	3.741	3.947	4.587	Y	4
4.742	4.694	4.188	3.025	1.836	1.621	1.349	.947	.417	0.0	Y	4
-4.437	-4.379	-4.194	-3.973	-3.747	-2.527	-2.301	-2.101	-1.976	-1.732	Y	4
-1.608	-1.402	-1.138	-.584	.020	.841	1.356	1.796	2.111	2.195	Y	4
0.000	1.468	2.720	3.104	3.366	3.764	3.973	4.178	4.564	5.204	Y	5
5.337	5.210	4.628	3.513	2.093	1.826	1.580	1.102	.599	.0	Y	5
-4.488	-4.356	-4.221	-4.049	-3.696	-2.527	-2.200	-1.996	-1.798	-1.580	Z	5
-1.402	-1.273	-.983	-.533	.071	1.069	1.763	2.278	2.644	2.781	Z	5
0.000	1.844	3.581	3.813	3.973	4.557	4.790	5.151	5.611	6.477	Y	6
6.530	6.457	5.646	3.868	2.144	1.877	1.585	1.186	.559	0.0	Y	6
-4.463	-4.338	-4.188	-4.089	-3.787	-2.189	-1.913	-1.689	-1.646	-1.608	Z	6
-1.430	-1.250	-.907	-.444	.094	1.041	1.811	2.428	3.000	3.213	Z	6
0.000	1.974	3.658	4.018	4.252	4.681	4.994	5.405	5.971	6.833	Y	7
6.990	6.916	6.132	4.049	2.169	1.979	1.709	1.237	.658	.000	Y	7
-4.463	-4.366	-4.214	-4.067	-3.739	-2.367	-1.913	-1.689	-1.674	-1.737	Z	7
-1.522	-1.306	-.988	-.470	.119	.937	1.681	2.403	2.949	3.137	Z	7
0.000	2.090	3.901	4.310	4.564	5.202	5.354	5.636	6.195	6.988	Y	8
6.988	6.988	6.325	4.232	2.065	1.862	1.504	1.021	.485	.000	Y	8
-4.437	-4.336	-4.190	-4.090	-3.601	-2.180	-1.970	-1.836	-1.785	-1.811	Z	8
-1.478	-1.199	-.942	-.587	.254	1.123	1.811	2.398	2.830	2.931	Z	8
29.528	33.798	33.337	35.560	38.100	40.640	43.815	48.578			XFUS	8
0.000	4.920	5.000	5.090	5.090	4.890	0.000	0.000	3.848	4.305	Y	1
4.536	5.258	5.946	6.965	6.967	5.977	4.450	3.104	2.062	1.763	Y	1
1.283	.574	.000								Y	1
-7.260	-7.250	-7.150	-7.090	-5.030	-4.920	-4.900	-4.427	-4.194	-4.094	Z	1
-3.739	-2.037	-1.760	-1.816	-1.181	-.871	-.658	-.168	.244	1.417	Z	1
2.131	2.720	2.901									
0.000	4.920	5.000	5.090	5.090	4.890	0.000	0.000	4.318	4.702	Y	A1

TABLE 3 (Continued)

4.851	5.436	6.025	6.995	7.000	5.908	4.506	3.211	1.966	1.671	Y	A1
1.194	.587	0.								Y	A1
-7.260	-7.250	-7.150	-7.090	-5.030	-4.920	-4.900	-4.637	-4.125	-3.950	Z	A1
-3.332	-2.096	-1.847	-1.831	-1.118	-.902	-.683	-.236	.259	1.333	Z	A1
2.002	2.469	2.601								Z	A1
0.000	4.920	5.000	5.090	5.090	4.890	0.000	0.000	5.154	5.283	Y	2
5.342	5.552	6.012	6.955	6.962	5.946	4.473	3.101	1.732	1.511	Y	2
1.110	.630	0.								Y	2
-7.260	-7.250	-7.150	-7.090	-5.030	-4.920	-4.900	-4.359	-4.021	-3.716	Z	2
-2.977	-2.370	-2.093	-1.951	-1.161	-1.074	-.780	-.310	.239	1.105	Z	2
1.694	2.004	2.113								Z	2
0.000	5.055	5.260	5.314	5.342	5.116	1.417	1.422	5.253	5.382	Y	A2
5.443	5.679	6.066	7.010	6.998	5.850	4.450	3.104	1.633	1.359	Y	A2
1.031	.551	0.								Y	A2
-7.396	-7.386	-7.287	-7.056	-4.889	-4.735	-4.737	-4.277	-3.970	-3.795	Z	A2
-2.979	-2.497	-2.273	-2.106	-1.189	-1.173	-.950	-.500	.005	.544	Z	A2
.930	1.242	1.326								Z	A2
0.000	4.956	5.210	5.314	5.331	5.128	2.761	2.766	5.263	5.441	Y	3
5.446	5.756	6.165	6.980	6.988	5.867	4.572	3.150	1.549	1.171	Y	3
.815	.411	.0								Y	3
-7.381	-7.419	-7.295	-7.117	-4.854	-4.750	-4.729	-4.171	-3.988	-3.861	Z	3
-3.175	-2.718	-2.492	-2.347	-1.328	-1.369	-1.232	-.787	-.267	-.036	Z	3
.173	.404	.406								Z	3
0.000	4.994	5.276	5.382	5.387	5.184	3.937	3.970	5.375	5.479	Y	A3
5.494	5.745	6.132	7.003	7.018	5.817	4.569	3.045	1.445	1.143	Y	A3
.787	.406	.000								Y	A3
-7.396	-7.417	-7.295	-7.041	-4.821	-4.717	-4.699	-4.138	-4.031	-3.853	Z	A3
-3.396	-3.015	-2.741	-2.550	-1.453	-1.539	-1.443	-1.039	-.582	-.399	Z	A3
-.216	-.081	.025								Z	A3
0.000	4.910	5.291	5.420	5.428	5.250	5.072	5.075	5.354	5.456	Y	4
5.494	5.662	6.020	6.988	6.993	5.720	4.448	2.438	1.346	1.041	Y	4
.658	.251	.000								Y	4
-7.432	-7.450	-7.525	-6.995	-4.780	-4.679	-4.676	-4.117	-4.092	-3.914	Z	4
-3.686	-3.381	-3.051	-2.878	-1.732	-1.829	-1.722	-1.257	-.947	-.818	Z	4
-.691	-.612	-.584								Z	4
0.000	5.100	5.306	5.484	5.819	5.819	5.819	5.845	5.870	5.870	Y	5
5.895	6.025	6.279	7.018	6.995	5.951	4.780	2.416	1.092	.838	Y	5
.592	.277	.000								Y	5
-7.432	-7.341	-7.188	-7.010	-4.719	-4.567	-4.467	-4.415	-4.389	-4.211	Z	5
-4.211	-3.780	-3.551	-3.373	-2.177	-2.225	-2.197	-1.786	-1.427	-1.402	Z	5
-1.402	-1.349	-1.349								Z	5
48.578	53.340	60.960	68.580	72.009	75.057	79.296	80.010	83.668	88.468	XFUS	10
0.000	.638	1.323	2.062	2.774	3.411	4.072	4.912	5.370	5.545	Y	1
5.842	6.325	6.985	6.982	6.574	6.116	5.479	4.768	4.003	3.366	Y	1
2.731	2.093	1.354	.615	.000						Y	1
-7.407	-7.429	-7.402	-7.399	-7.396	-7.394	-7.391	-7.363	-7.132	-6.393	Z	1
-4.178	-3.515	-3.360	-2.189	-2.192	-2.217	-2.220	-2.172	-2.073	-1.948	Z	1
-1.849	-1.671	-1.471	-1.397	-1.349						Z	1
0.000	.691	1.303	1.989	2.753	3.261	3.846	4.762	5.728	5.979	Y	2
6.431	6.657	7.041	7.036	6.474	5.941	5.329	4.516	3.828	3.241	Y	2
2.553	1.943	1.280	.643	.000						Y	2
-7.305	-7.277	-7.300	-7.272	-7.267	-7.267	-7.264	-7.234	-6.772	-6.134	Z	2
-4.453	-3.970	-3.815	-2.543	-2.455	-2.373	-2.304	-2.236	-2.112	-2.044	Z	2
-1.920	-1.893	-1.783	-1.646	-1.577						Z4	2
0.000	.457	1.095	1.857	2.672	3.284	3.995	4.938	5.674	6.058	Y	3
6.388	6.695	7.026	7.026	6.307	6.172	5.804	5.116	4.582	4.097	Y	3
2.850	1.943	1.374	0.643	0.0						Y	3
-7.254	-7.254	-7.254	-7.229	-7.254	-7.254	-7.280	-7.279	-7.063	-6.652	Z	3
-6.035	-4.557	-4.506	-3.155	-3.086	-2.550	-2.195	-2.126	-2.071	-2.044	Z	3
-1.934	-1.900	-1.852	-1.845	-1.838						Z	3
0.000	0.457	1.095	2.233	3.251	4.674	5.441	5.977	6.363	6.594	Y	4
6.721	6.858	7.053	7.032	6.721	6.580	6.447	6.173	5.500	4.000	Y	4
2.736	1.999	1.313	0.625	0.0						Y	4
-7.178	-7.178	-7.178	-7.178	-7.178	-7.178	-7.178	-7.063	-6.610	-6.172	Z	4
-5.486	-4.897	-4.894	-3.876	-3.840	-2.743	-2.332	-2.085	-2.030	-2.030	Z	4
-2.030	-2.030	-2.030	-2.030	-2.030						Y	4

TABLE 3 (Continued)

```
0.000   0.274   0.521   5.212   5.418   5.692   5.829   5.900   6.172   6.584     Y      5
6.858   6.858   6.980   6.995   6.858   6.721   6.584   6.447   6.172   5.898     Y      5
5.692   5.555   5.418   5.349   0.0                                               Y      5
-7.132  -7.132  -7.132  -7.132  -7.132  -7.132  -7.132  -7.102  -6.995  -6.515    Z      5
-5.486  -5.349  -5.102  -4.211  -3.978  -3.018  -2.606  -2.332  -2.126  -2.057    Z      5
-2.057  -2.057  -2.057  -2.057  -2.057                                            Z      5
0.000   0.274   0.521   5.212   5.418   5.692   5.829   5.900   6.104   6.378     Y      6
6.652   6.830   6.858   6.830   6.652   6.378   6.241   6.104   5.966   5.829     Y      6
5.692   5.555   5.418   5.349   0.000                                             Y      6
-7.132  -7.036  -6.721  -6.721  -6.970  -7.164  -7.187  -7.180  -7.094  -6.788    Z      6
-6.152  -5.000  -4.595  -4.000  -3.038  -2.402  -2.219  -2.096  -2.026  -2.003    Z      6
-2.026  -2.096  -2.219  -2.330  -2.330                                            Z      6
0.000   0.274   0.411   5.109   5.246   5.384   5.658   5.795   5.932   6.206     Y      7
6.481   6.618   6.769   6.700   6.481   6.400   6.206   6.206   5.932   5.795     Y      7
5.658   5.384   5.200   5.116   0.000                                             Y      7
-6.789  -6.584  -6.241  -6.298  -6.578  -6.770  -6.972  -6.995  -6.972  -6.770    Z      7
-6.298  -5.879  -4.595  -3.700  -2.891  -2.700  -2.420  -2.420  -2.218  -2.195    Z      7
-2.218  -2.420  -2.700  -2.880  -2.880                                            Z      7
0.000   0.274   0.411   5.047   5.246   5.384   5.658   5.795   5.932   6.069     Y      8
6.344   6.618   6.755   6.618   6.344   6.344   6.069   5.932   5.932   5.795     Y      8
5.658   5.521   5.246   5.144   0.000                                             Y      8
-6.721  -6.515  -6.200  -6.200  -6.633  -6.832  -7.039  -7.064  -7.039  -6.694    Z      8
-6.633  -5.899  -4.663  -3.428  -2.694  -2.694  -2.363  -2.288  -2.288  -2.263    Z      8
-2.288  -2.363  -2.694  -2.949  -2.949                                            Z      8
0.000   0.000   0.000   5.322   5.384   5.520   5.658   5.795   5.932   6.069       Y    9
6.206   6.344   6.447   6.344   6.206   6.206   6.069   5.932   5.932   5.795     Y      9
5.658   5.521   5.384   5.349   0.0                                               Y      9
-6.035  -6.035  -6.035  -6.035  -6.137  -6.399  -6.540  -6.584  -6.539  -6.399    Z      9
-6.137  -5.667  -4.595  -3.522  -3.053  -3.053  -2.791  -2.650  -2.650  -2.606    Z      9
-2.650  -2.791  -3.053  -3.155  -3.155                                            Z      9
0.000   0.000   0.000   5.795   5.795   5.795   5.795   5.795   5.795   5.795     Y     10
5.795   5.795   5.795   5.795   5.795   5.795   5.795   5.795   5.795   5.795     Y     10
5.795   5.795   5.795   5.795   0.000                                             Y     10
-5.857  -5.857  -5.857  -5.857  -5.857  -5.857  -5.857  -5.857  -5.857  -5.857    Z     10
-5.857  -5.857  -4.595  -3.333  -3.333  -3.333  -3.333  -3.333  -3.333  -3.333    Z     10
-3.333  -3.333  -3.333  -3.333  -3.333                                            Z     10
 39.091  2.743 -8.227 0.                                                          NACEL  1
 .0000 1.3716 2.7430 4.1150 5.4860 6.8560 8.2300 9.6010 10.973 12.344             NACE1 X1
13.716 15.088 16.459 17.831 19.202 20.574 21.946 23.317 24.687                    NACE1 X2
0.0000 0.3545 0.5190 0.5845 0.5845 0.5845 0.6335 0.7535 0.8475 0.8475             NACE1 R1
0.8475 0.8475 0.8475 0.8475 0.7740 0.6240 0.4380 0.2680 0.0000                    NACE1 R2
 62.438 16.665 -4.795 0.
 .0000 1.3716 2.7430 4.1150 5.4860 6.8560 8.2300 9.6010 10.973 12.344             NACE2 X1
13.716 15.088 16.459 17.831 19.202 20.574 21.946 23.317 24.687                    NACE2 X2
0.0000 0.3545 0.5190 0.5845 0.5845 0.5845 0.6335 0.7535 0.8475 0.8475             NACE2 R1
0.8475 0.8475 0.8475 0.8475 0.7740 0.6240 0.4380 0.2680 0.0000                    NACE2 R2
76.789 34.629 -3.335
0.000   0.6808 1.3716 2.332  3.0    3.7    4.4    5.1    5.8    6.5               NACEL  3
7.2     7.9    8.6    9.3    10.0   10.7   11.4   12.1   12.779                   NACE3 X2
0.000   0.238  0.300  0.339  0.339  0.339  0.339  0.339  0.339  0.339             NACE3 R1
0.339   0.339  0.339  0.339  0.339  0.339  0.339  0.339  0.339                    NACE3 R2
 67.628 20.574 -3.335 15.240 90.963 20.574  6.193  4.762                          FINORG
0.0     20.    30.    40.    50.    60.    70.    80.    90.    100.              XFIN
0.0     .695   .938   1.111  1.215  1.250  1.172  .938   .547   .0                FINORD
 70.564 20.574 -5.918 10.922 67.008 20.574 -3.37  15.240                          FINORG2
0.0     20.    30.    40.    50.    60.    70.    80.    90.    100.              XFIN
0.0     .70    .933   1.116  1.216  1.250  1.167  .933   .55    0.0               FINORD2
```

TABLE 4 - DRAG COEFFICIENTS OF NASA SUPERCRUISER 4

DRAG COEFF. / SOURCES / M_∞	1.2			1.6			1.8		
	Calculated		Experimental	Calculated		Experimental	Calculated		Experimental
DRAG TYPE	DTNSRDC	NASA	NASA	DTNSRDC	NASA	NASA	DTNSRDC	NASA	NASA
Skin Friction	0.00920	0.00936	-	0.00872	0.00872	-	0.00840	0.00840	-
Near-Field Wave Drag	0.01032	0.00838	-	0.00647	0.00635	-	0.00600	0.00600	-
Drag due to Camber	0.00170*	0.00170	-	0.00310*	0.00310	-	0.00360*	0.00360	-
Total Drag Coefficient	0.02122	0.01944	0.0198	0.01829	0.01817	0.0186	0.01800	0.01800	0.0181

* Not calculated at DTNSRDC, instead, NASA values were used for camber corrections

TABLE 5 - DRAG COEFFICIENTS OF SUPERSONIC V/STOL CONFIGURATION WITH VARIOUS STORE ARRANGEMENTS AT ZERO LIFT

M_∞	C_D VALUES / TYPE OF C_D / AIRCRAFT	NASA SUPERSONIC CRUISE FIGHTER	V/STOL AIRCRAFT 1	V/STOL WITH 2 MRAAM 2	V/STCL WITH 4 MRAAM 3	V/STCL WITH 4 MRAAM 3A	V/STOL WITH 2 TANKS T	V/STOL WITH 4-MRAAM 2 SRAAM 5	V/STOL WITH 2-MRAAM 2 SRAAM 6	V/STOL WITH 4-MRAAM 2 TANKS 7	V/STOL WITH 1 ECM 2 TANKS 8	V/STOL WITH 1 ECM 2 SRRAM 9	V/STOL WITH 2 ASM 2 SRRAM 10
1.8	C_D(wave,far)	0.01005	0.01107	0.01122	0.01146		0.01495	0.01143					0.01154
	C_D(wave,near)	0.00960	0.01065	0.01079	0.01102	0.01140	0.01438	0.01099		0.01571			0.01110
	C_D(friction)	0.00840*	0.00496	0.00513	0.00531	0.00531	0.00544	0.00533	0.00516	0.00575	0.00575		0.00531
	C_D(total)	0.01800	0.01561	0.01592	0.01633	0.01671	0.01982	0.01632		0.02146			0.01641
	C_D(experitment)	0.01810											
1.6	C_D(wave,far)		0.01154	0.01173	0.01210								0.01226
	C_D(wave,near)	0.00957	0.01114	0.01132	0.01168	0.01209							0.01184
	C_D(friction)	0.00872*	0.00527	0.00545	0.00564	0.00564	0.00577	0.00567	0.00549	0.00612	0.00612		0.00564
	C_D(total)	0.01829	0.01641	0.01677	0.01732	0.01773							0.01748
	C_D(experiment)	0.01860											
1.2	C_D(wave,far)		0.01416	0.01372	0.01429								0.01521
	C_D(wave,near)	0.01202	0.01241	0.01202	0.01252								0.01333
	C_D(friction)	0.00920*	0.00594	0.00615	0.00635	0.00635	0.00651	0.00638	0.00617	0.00688	0.00688		0.00636
	C_D(total)	0.02122	0.01835	0.01817	0.01887								0.01969
	C_D(experiment)	0.01980											
0.6	C_D(friction)	0.01010*											
	C_D(experiment)	0.01260											
0.3	C_D(friction)		0.00624				0.00681	0.00675	0.00653	0.00728	0.00728		0.00669
	C_D(experiment)												
0.2	C_D(friction)		0.00664				0.00725	0.00719	0.00695	0.00776	0.00775		0.00712
	C_D(experiment)												
0.1	C_D(friction)		0.00739				0.00807	0.00799	0.00773	0.00862	0.00862		0.00792
	C_D(experiment)												

* Calculated based on $Re_\infty = 2 \times 10^6$. All other skin friction values were calculated based on $\bar{c}$ = 31.06 feet (9.47 meters) at h = 50,000 feet (15,240 meters). Skin friction values for Mach 0.1, 0.2, and 0.3 were computed based on the same mean chord length at h = 1,000 feet (304.8 meters).

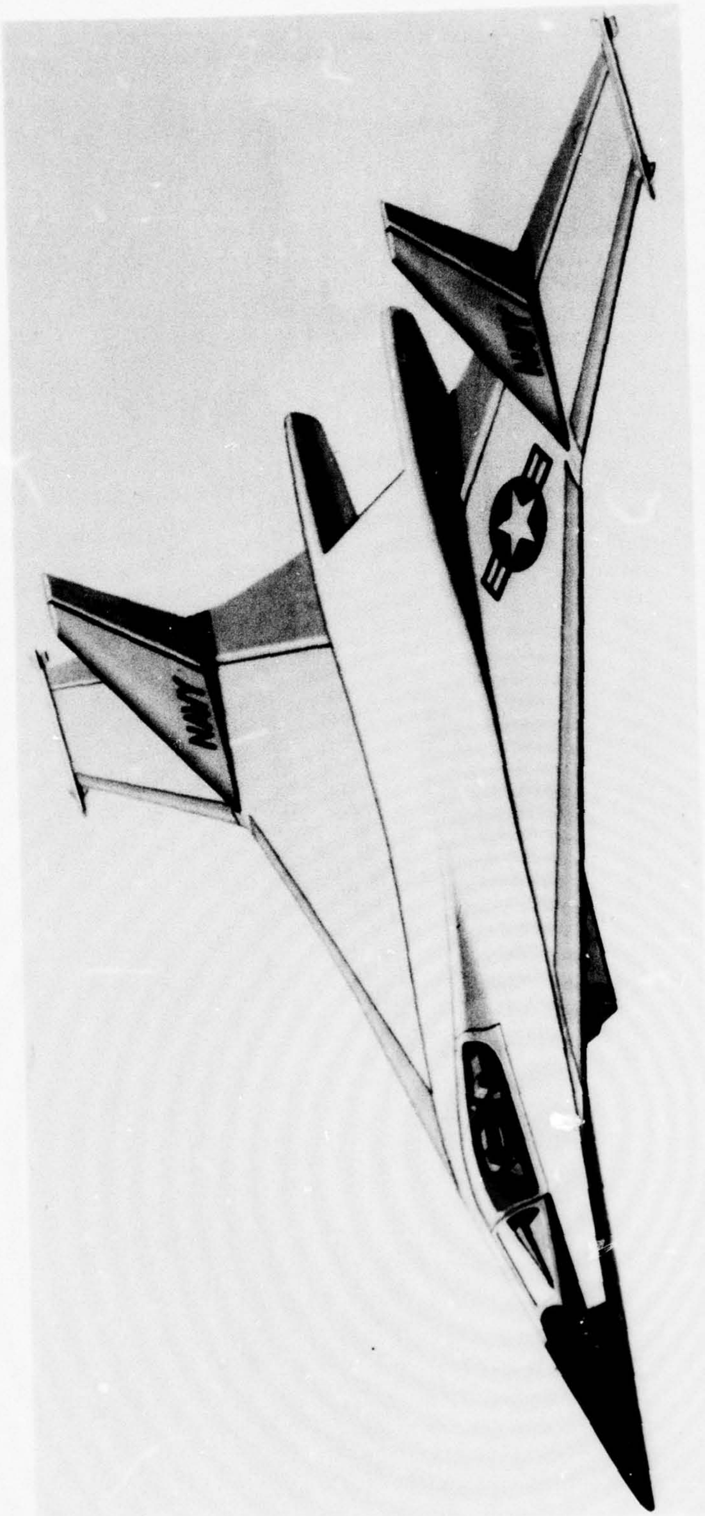

Figure 1 - An Isometric View of the Modified Aircraft Configuration

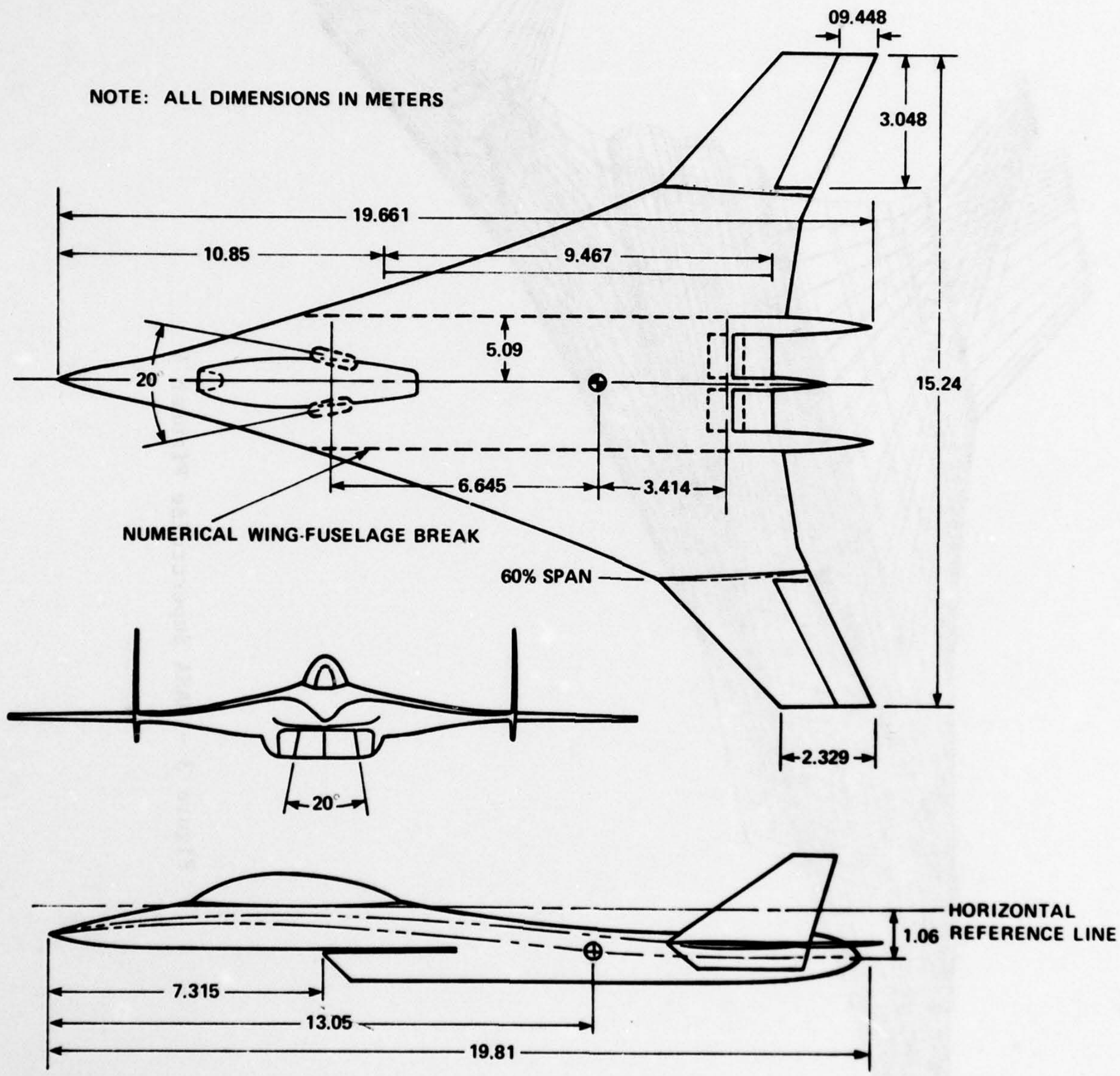

Figure 2 - Three Views of the Aircraft Configuration

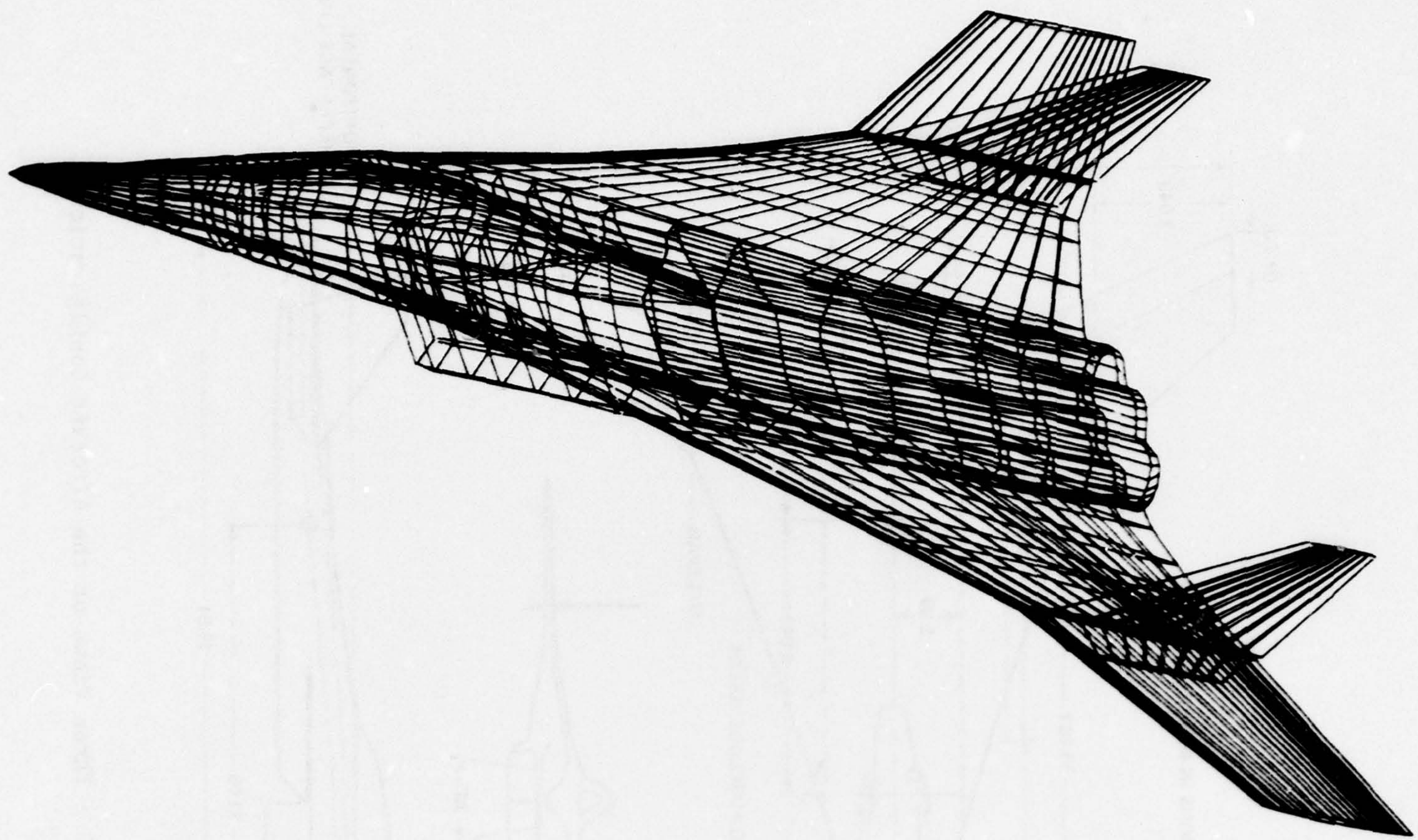

Figure 3 - NASA Supercruise Fighter 4

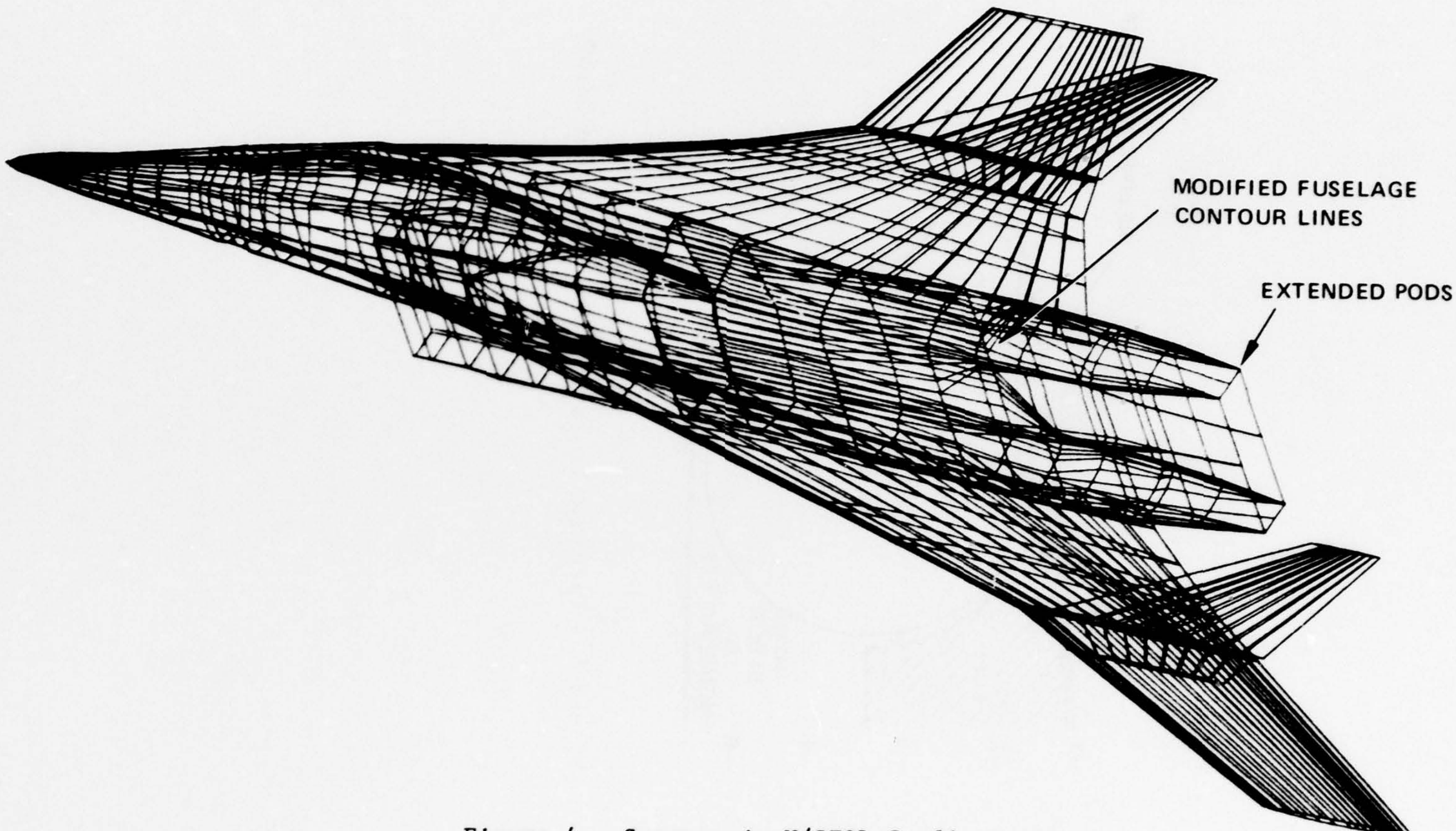

Figure 4 - Supersonic V/STOL Configuration
(Modified from NASA Supercruise Fighter 4)

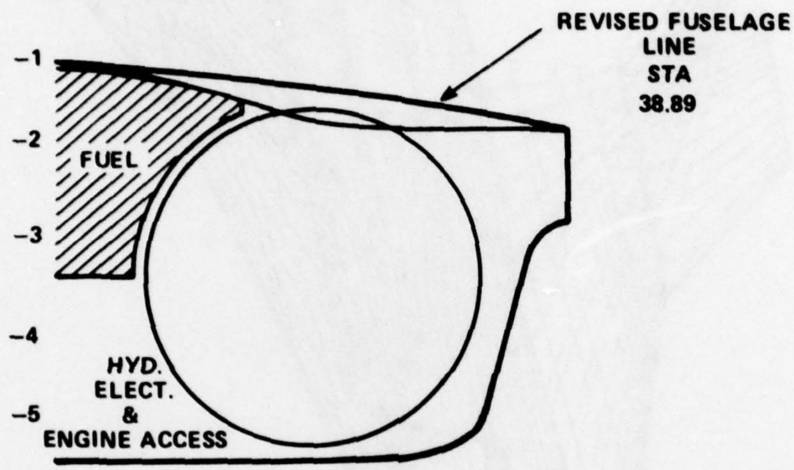

Figure 5 - Fuselage Cross Section at Station 38.89

Figure 6 - Orthographic View of Supersonic V/STOL Configuration with Various Store Arrangements

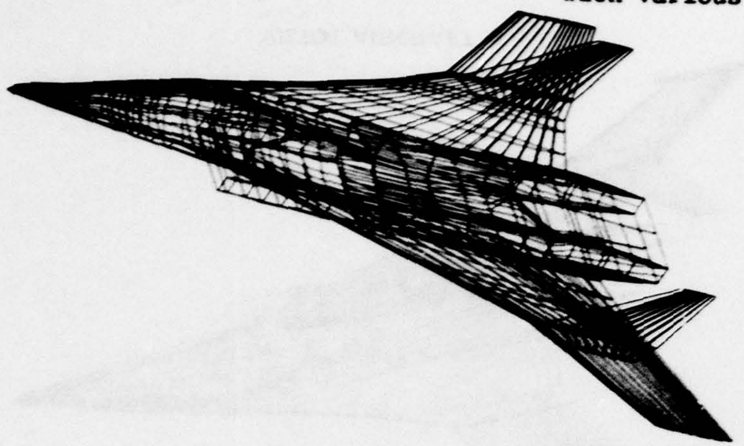

V/STOL AIRCRAFT 1

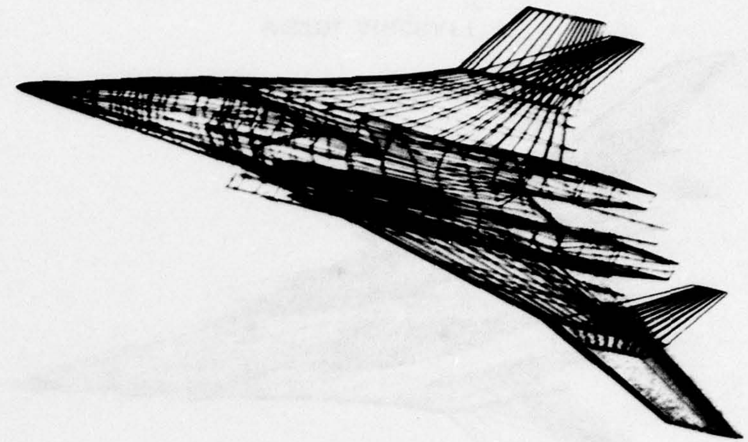

V/STOL AIRCRAFT 2

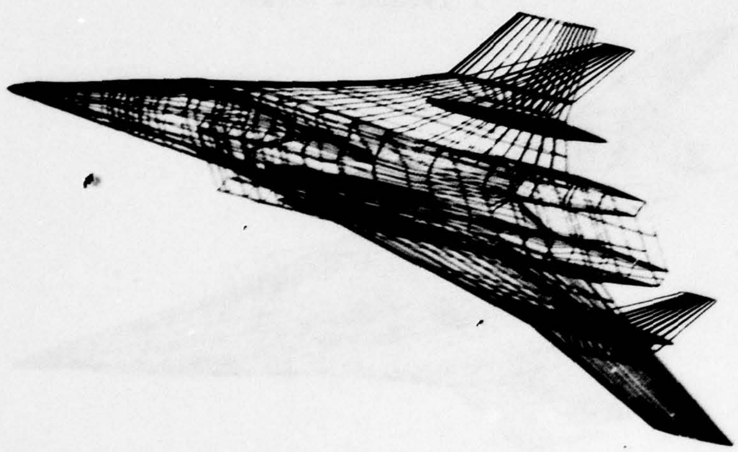

V/STOL AIRCRAFT 3

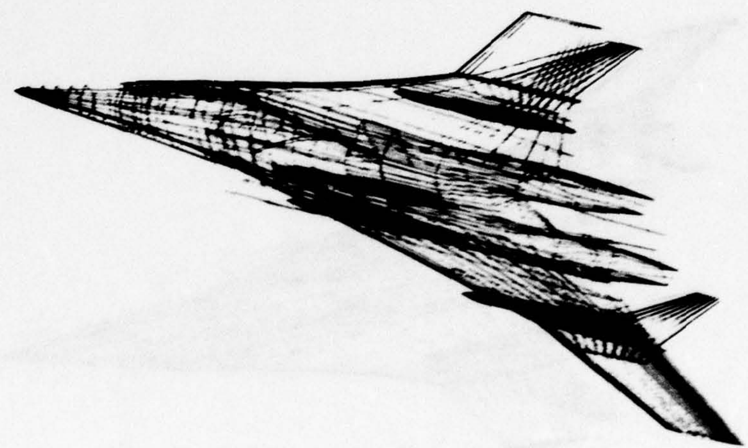

V/STOL AIRCRAFT 3A

Figure 6 (Continued)

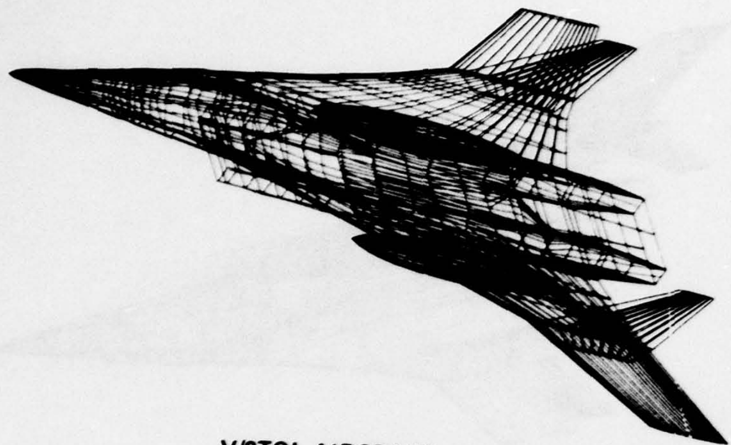

V/STOL AIRCRAFT T

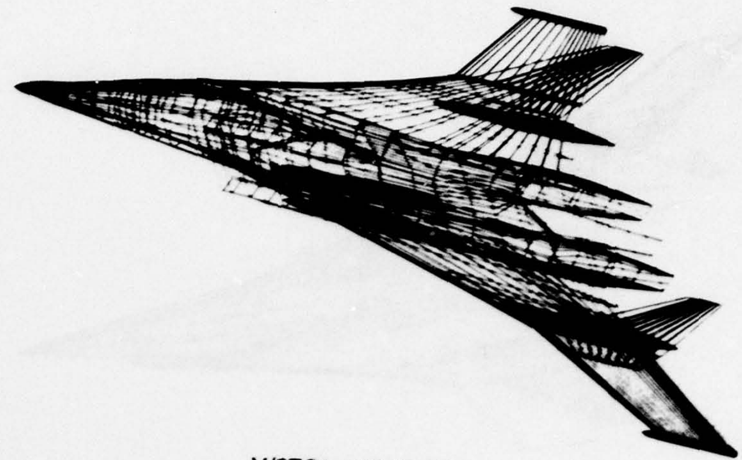

V/STOL AIRCRAFT 5

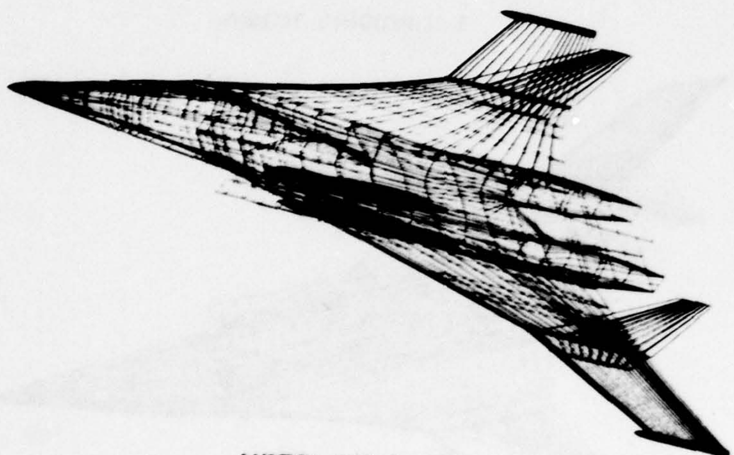

V/STOL AIRCRAFT 6

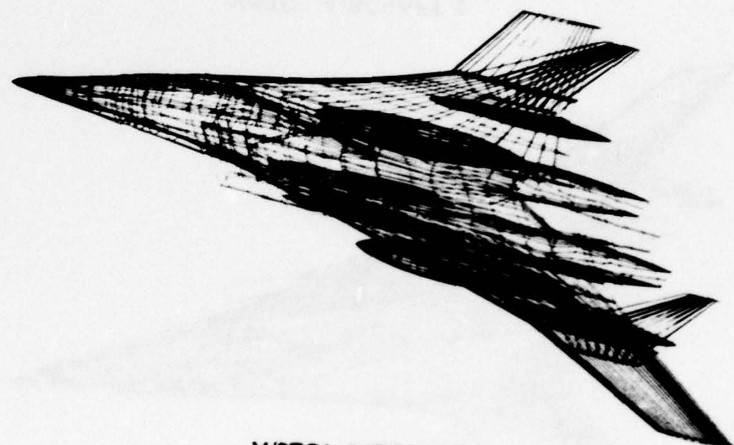

V/STOL AIRCRAFT 7

Figure 6 (Continued)

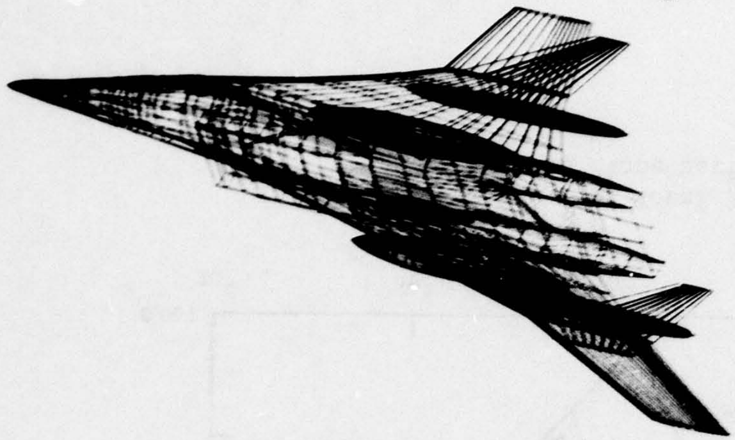

V/STOL AIRCRAFT 8

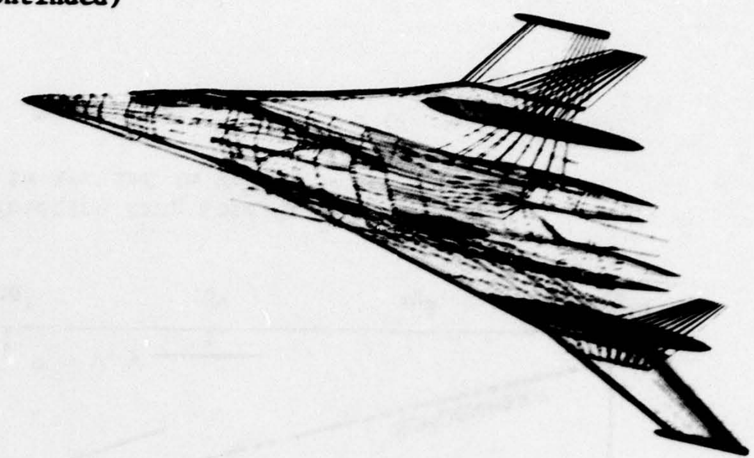

V/STOL AIRCRAFT 9

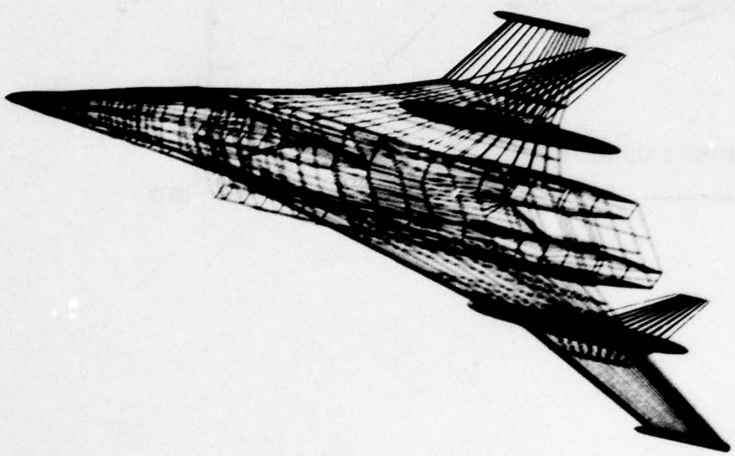

V/STOL AIRCRAFT 10

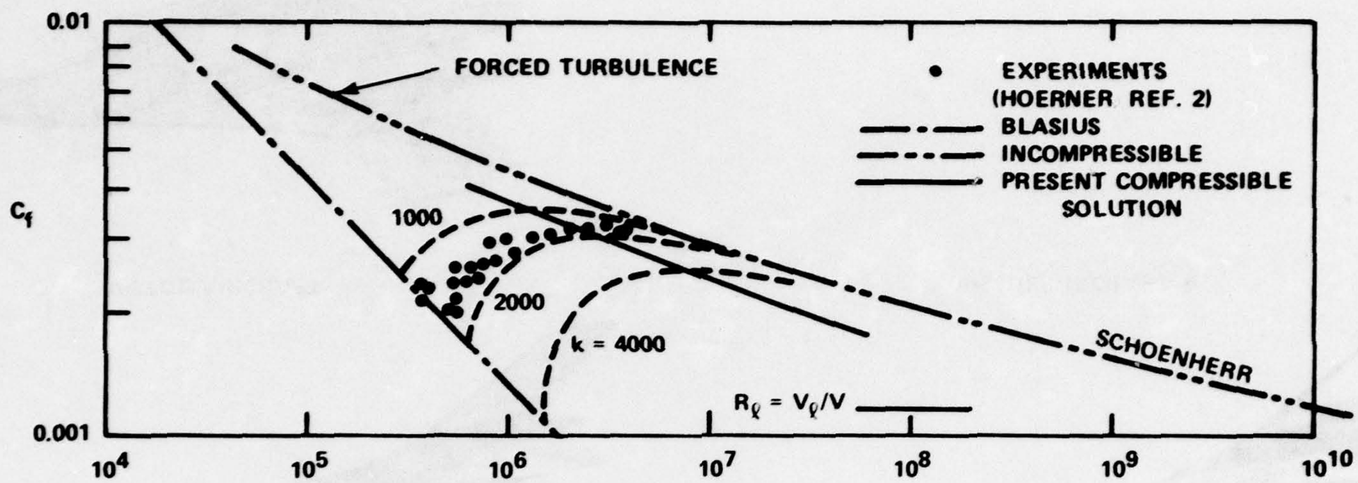

Figure 7 - Average or Total Skin-Friction Drag Coefficient of Smooth and Plane Surfaces in Air and in Water

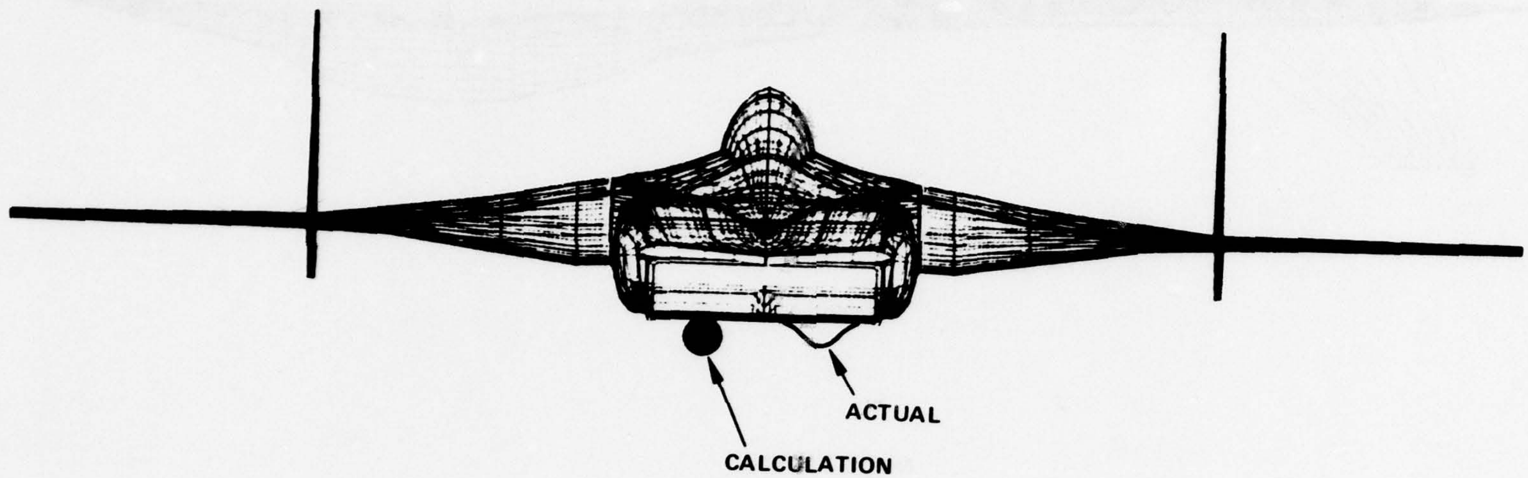

Figure 8 - Store Drag Calculation Method

Figure 8 (Continued)

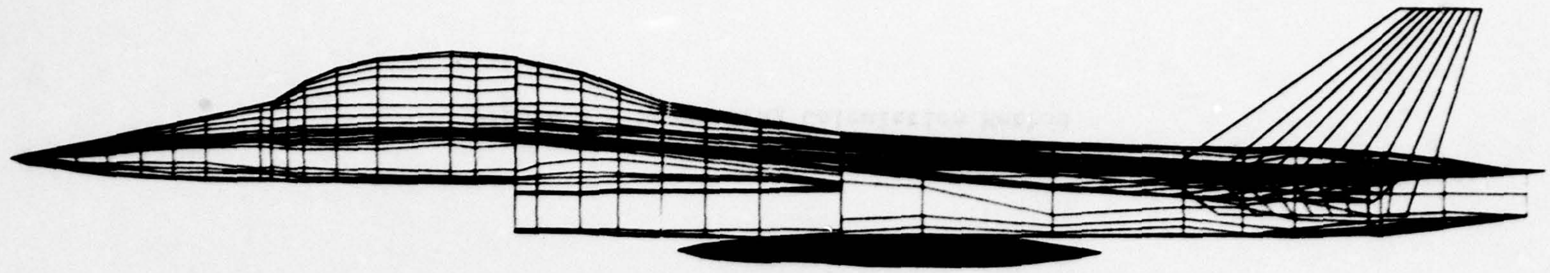

CALCULATION

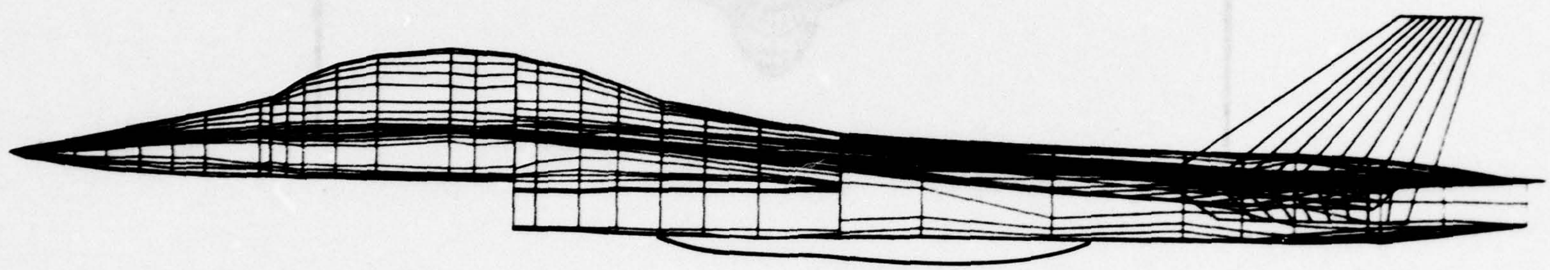

ACTUAL

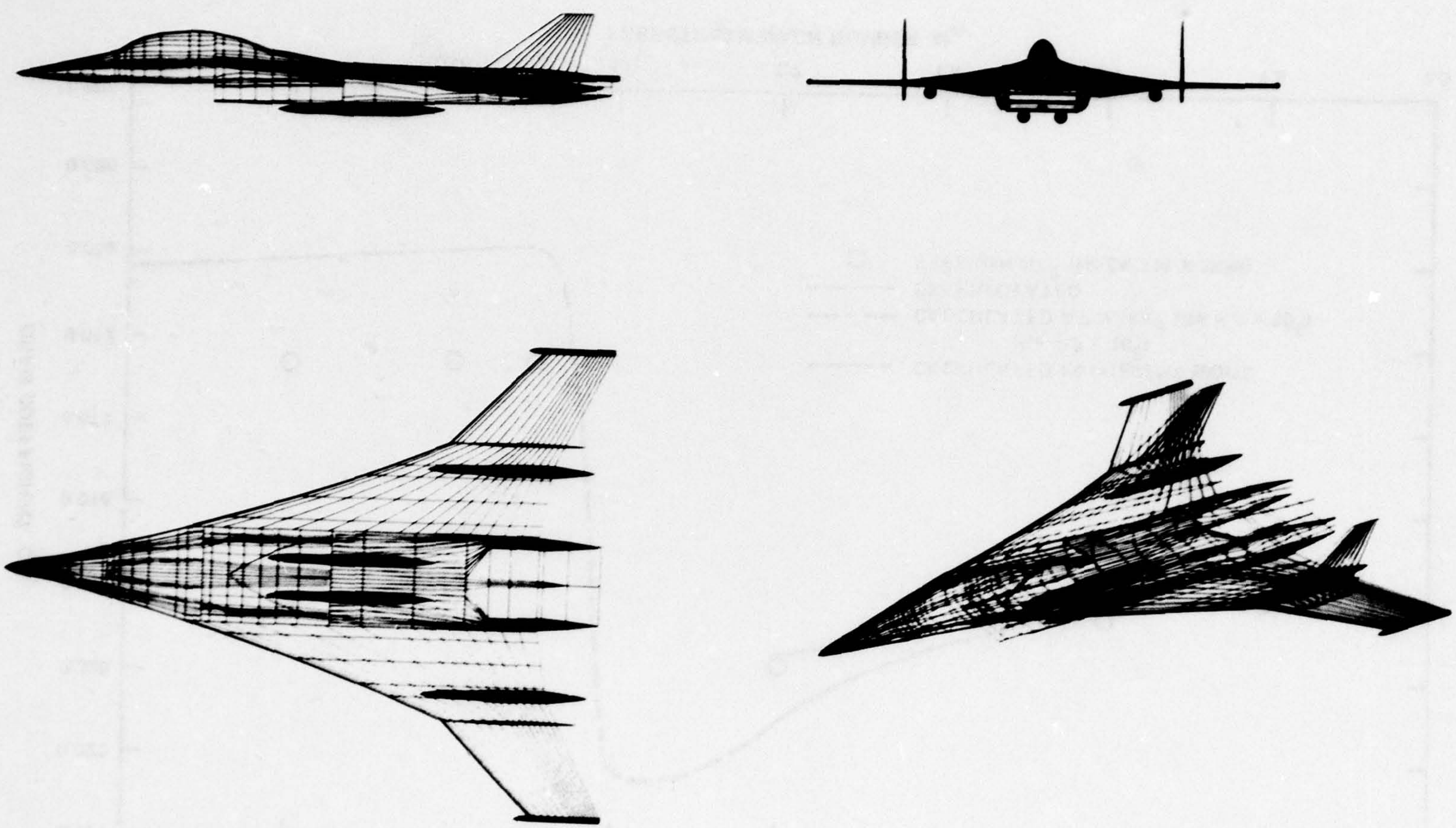

Figure 9 - Oblique Orthographic Views of V/STOL Configuration 5

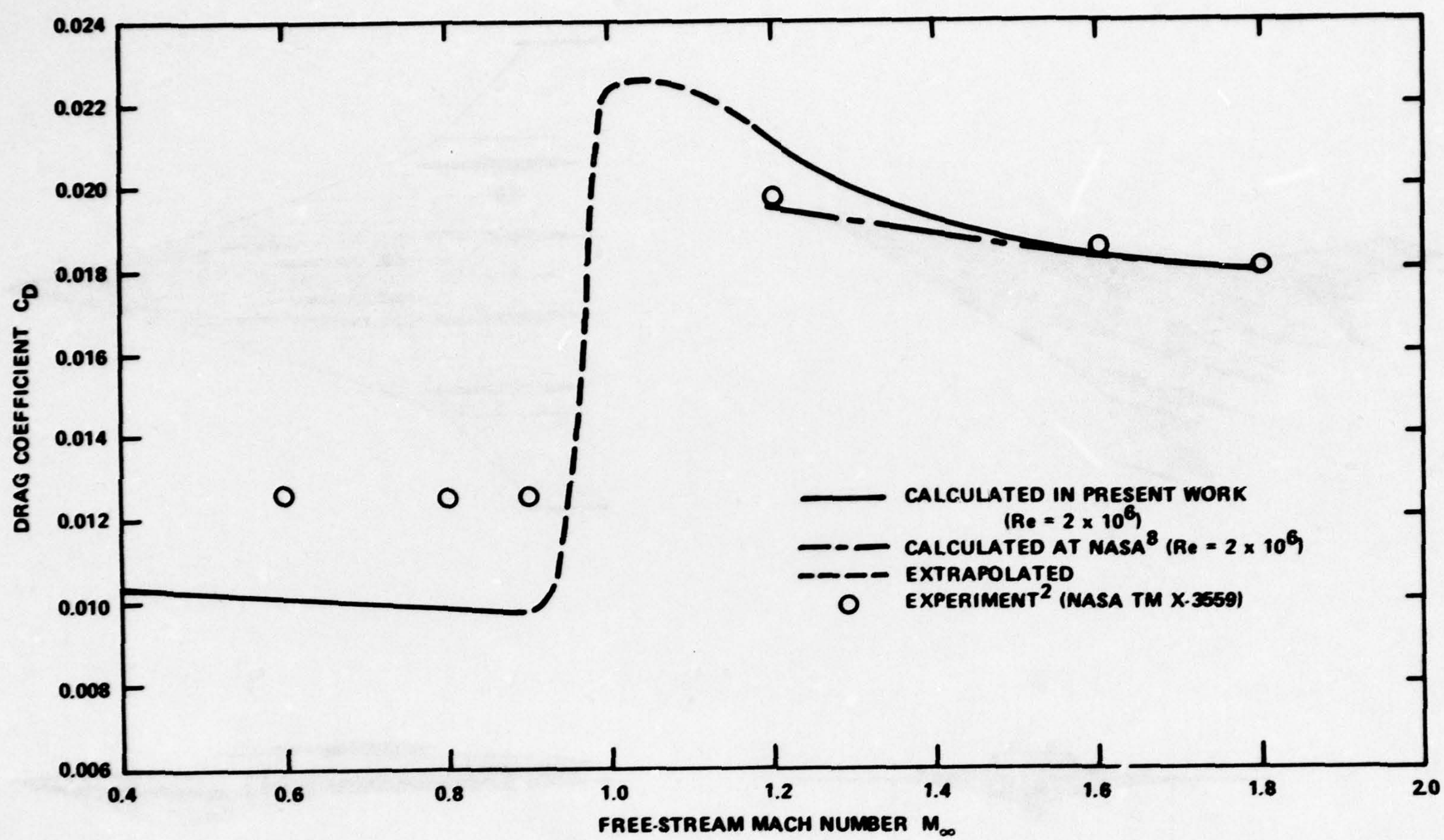

Figure 10 - Drag Coefficient of NASA Supercruiser 4 at Zero Lift

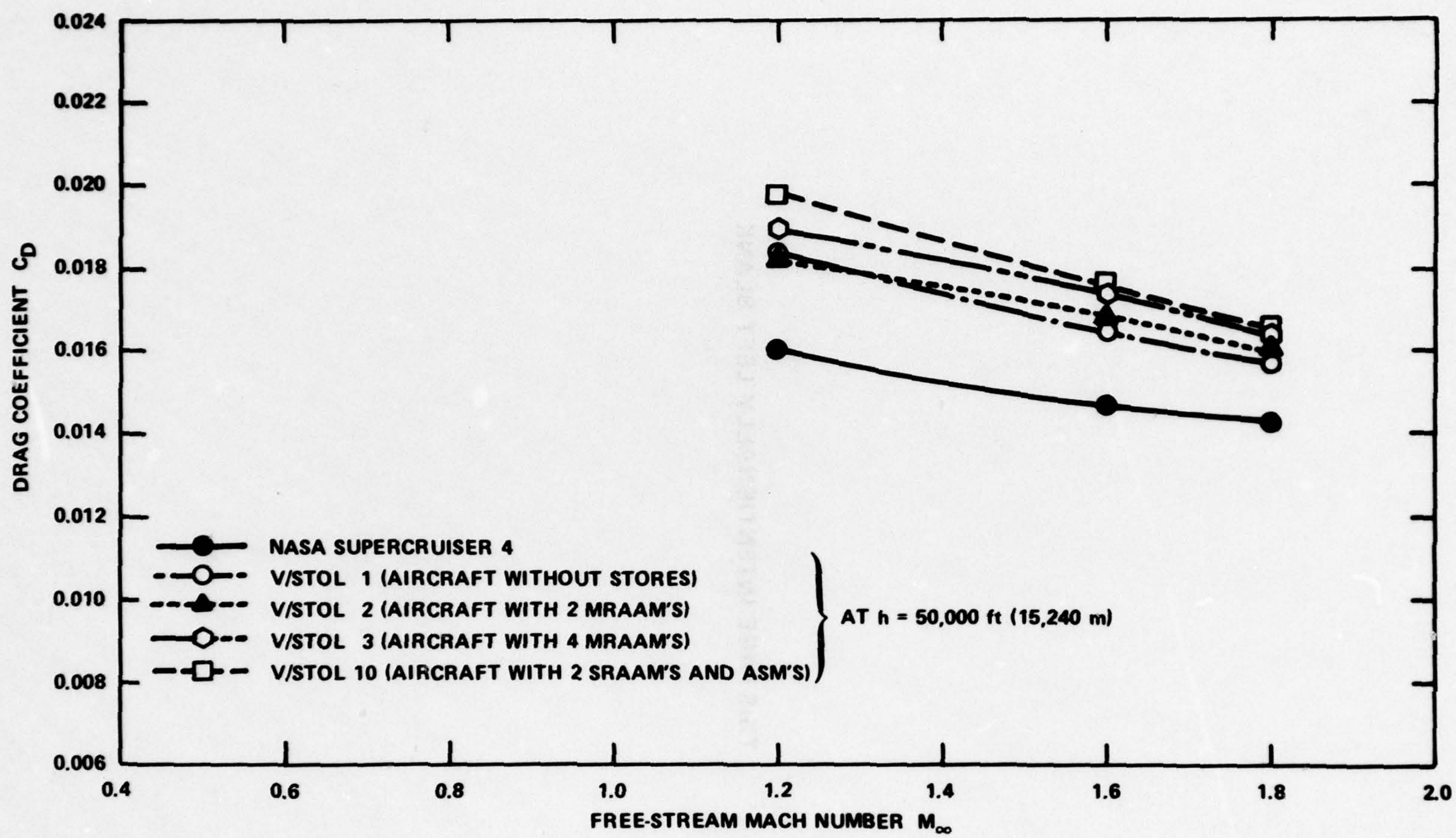

Figure 11 - Drag Coefficients of a V/STOL Configuration with Typical Store Arrangements

INITIAL DISTRIBUTION

Copies		Copies	
4	CNR 1 211 1 430B 1 432 1 438	12	DDC
		1	AFOSR
		1	USAFA
1	NRL	1	AF INST TECH
4	ONR 1 Boston 1 Chicago 1 London, England 1 Pasadena	1	AFASD/Dayton (XRL)
		1	AFFDL (FXMB)
		1	AEDC
1	USNA	5	NASA 1 HQ, Washington, D.C. (RHT-5) 2 Ames Research Center/Lib MS-285 MS-286 1 Langley Research Center 1 Lewis Research Center MS-500-307
1	USNPGSCOL		
5	NADC 1 AIR 07 3 AIR IV3, W. Miller 1 AIR 3015, C. Mazza		
1	NWC/China Lake Code 124	1	U of Akron/Lib
1	NSWC/Dahlgren	1	Brown U/Div of Engr
1	NSWC/White Oak	2	Calif Inst of Tech 1 Grad Aero Labs 1 Dr. T. Kubota
17	NAVAIRSYSCOM 1 AIR 03A 1 AIR 03C 1 AIR 03E 1 AIR 03PA 1 AIR 03PA3 1 AIR 310 3 AIR 320D 1 AIR 5108 1 AIR 530B 4 AIR 5301 1 AIR 954 1 PMA 269	1	Calif Inst of Tech/Jet Prop Lab
		2	U of Calif/Berkeley 1 Prof. M. Holt/Div Aero Sciences 1 Lib
		1	U of Calif/L.A.
		1	U of Calif/LaJolla
1	NAVSEASYSCOM	1	U of S Calif/Lib
1	NAVAIRPROPTESTCEN Code PE43, C.L. Palcza	1	Catholic U of America/Lib

Copies		Copies	
1	U of Cincinnati/ Aerospace Engr	1	U of Virginia/Alderman Lib
2	Clemson U 1 Dr. T. Yang/Mech Engr Dept 1 Lib	2	Virginia Polytech Inst 1 Carol M. Newman Lib 1 Aero & Ocean Engr
		1	U of Washington/Lib
1	Cornell U/Lib	1	W Virginia U/Dept Aero Engr
1	Georgia Inst Tech/Lib	1	American Inst of Aeronautics & Astronautics
1	Harvard U/Gordon McKay Lib	1	Advanced Tech Ctr/C. Haight
1	John Hopkins U/Lib	1	ARO Inc/Lib
1	U of Illinois/Lib	1	Bell Aerospace
2	U of Maryland 1 Aerospace Engr 1 Lib	1	Boeing Company/Seattle G. Lampard
		1	Calspan Corp/Buffalo
1	MIT/Lib	1	Douglas Aircraft Co/Lib
2	U of Michigan 1 Aerospace Engr 1 Lib	1	Flow Research/Kent Washington
		1	General Dynamics Convair/Lib
1	New York U/Courant Inst Math Sci	1	General Dynamics, Fort Worth D. Lobrecht
1	U of N Carolina/Lib	1	Grumman Aerospace Corp/Lib R. Kress
2	N Carolina State U/Raleigh 1 Dr. F.R. DeJarnette/Mech & Aerospace Engr Dept 1 Lib	1	Inst for Defense Analyses
		1	Lockheed-California A. Burns
1	Pennsylvania State U/Lib		
1	Princeton U/Lib	1	Lockheed-Georgia Co/Lib
1	Purdue U/Lib	1	Lockheed Missiles & Space Co/Lib
1	Stanford U/Lib	1	LTV Aerospace Corp/Lib
1	U of Tennessee Space Inst		

Copies	
1	McDonnell Douglas St. Louis/R. Anderson
1	Nielsen Engr & Res Inc
1	Northrop Aircraft/O. Lewis
1	Pratt & Whitney E. Lehman
1	Rockwell International Corp/M. Debenport
1	TRW Systems Group/Lib
1	Vought Corp/H. Driggers

CENTER DISTRIBUTION

Copies	Code	Name
1	012	
1	11	
1	15	
1	18	
1	27	
1	28	
10	5211.1	Reports Distribution
1	522.1	Library (C)
1	522.2	Library (A)
2	522.3	Aerodynamics Lib